



# **Design Note TRI-DN-13-29**

## **e-Linac 100 kW Tuning Beam Dump Local and Upstream (EHDT beamline) Shielding Design**

**Document Type:** Design Note

**Release:** 02                   **Release Date:** 2014/04/04

**Author(s):** Mina Nozar

	Name:	Signature:	Date:
<b>Author:</b>	Mina Nozar		3 Apr 2014
<b>Reviewed By:</b>	Isaac Earle		APRIL 4, 2014
	Shane Koscielniak		2014/Apr/04
	Anne Trudel		
<b>Approved By:</b>	Anne Trudel		2014/04/04

*Note: Before using a copy (electronic or printed) of this document you must ensure that your copy is identical to the released document, which is stored on TRIUMF's document server.*

e-Linac 100 kW Tuning Beam Dump Local and Upstream (EHDT beamline) Shielding  
Design

Document-103968

Release No. 02

Release Date.: 2014/04/04

**History of Changes**

<b>Release Number</b>	<b>Date</b>	<b>Description of Changes</b>	<b>Author(s)</b>
#01	2013-12-05	Initial release	Mina Nozar
#02	2014-04-04	Title change	Mina Nozar
		Updated simulation results for the final Beam Dump insert	Mina Nozar
		Final design of the EHDT shielding configuration and simulation results for the EHDT	Mina Nozar

# e-Linac 100 kW Tuning Beam Dump local and upstream (EHDT beamline) Shielding Design

**TRI-DN-13-29  
Document # 103968**

Mina Nozar  
Mar 31, 2014

This report summarizes simulation results of the final shielding configuration considered for the ARIEL 100 kW Beam Dump, using FLUKA [Ref. 1, 2]. The shielding design was divided into two stages: 1) local shielding, 2) upstream shielding. Local shielding design was finalized first since the upstream shielding depends on the local shielding material, configuration, and size. At the initial stages of the studies, two beam settings were considered for each shielding configuration examined: 1) 75 MeV, 1.33333 mA, 2) 25 MeV, 4 mA. Because the former resulted in higher radiation fields, we focused on this beam setting for the remainder of the investigations to determine best shielding material and configuration, prompt and residual dose rates, and activities in different components of the BD and BD Local shielding. Various shielding materials and configurations were examined for the local shielding in an effort to find an optimum solution to attenuate radiation levels to acceptable levels. Results shown here are mostly for the final set of configurations of the BD bulk and EHDT (High Energy Dump Transfer) beamline bulk and close-in collimation style shielding.

# Table of Contents

Shielding Requirements .....	1
Factors Considered in Choosing Shielding Material & Configuration.....	2
Geometry & beam setup in FLUKA.....	7
Beam Dump Parameters.....	7
Beam Specifications.....	7
Coordinate System Definition.....	7
Wall Thicknesses.....	7
Simulation Results for the Final Local BD Shielding Configuration (lead + steel/concrete).....	16
Quantitative Values for Dose Rates Outside of the BD Local Shielding.....	20
Residual Dose Rates.....	24
Activation Results.....	25
Deposited Power Distribution in the BD BD cooling water, and BD Shielding Components.....	31
EHDT Shielding Results – Bulk Shielding .....	33
EHDT Shielding Results – Additional Shielding Upstream of the EHDT Bulk Shielding.....	35
Conclusions.....	43
Acknowledgements.....	44
References.....	44

## Shielding Requirements

Required dose rate levels are given in Table 1 for the 100 kW Beam Dump (BD). More details are given in [Ref 3,4].

*Table 1: Dose rate limits necessary to meet the requirements.*

Direction	Above	Below	West (0°)	East	North (90°)	South
Limits (mSv/h)	10 at 3 m from beamline	10 at wall & soil	10 at wall & soil	3 AQAP <sup>1</sup>	10 at wall & soil	3 at 3 m from beamline

## Factors Considered in Choosing Shielding Material & Configuration

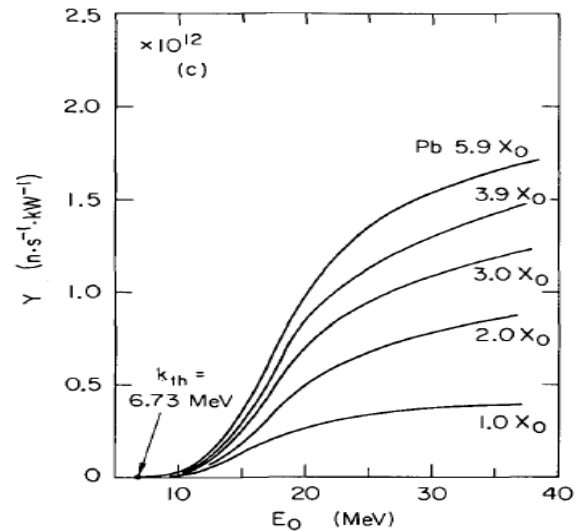
Traditionally, shielding radiation from 75 MeV electron beam, involves an inner layer of a high density (high Z) material to absorb the electromagnetic cascades from electrons interacting in the target material, followed by a light material to reduce the energy of neutrons emanating from the material. Electron threshold energies for neutron production are 13.03 MeV for Al, 9.91 MeV for Cu, and 6.73 MeV for Pb. For Fe/steel, the threshold is close to that for Cu. With 75 MeV incident electrons, we are well above the ( $\gamma, n$ ) threshold in the above materials and therefore need to deal with the added complication of shielding the generated neutrons.

Fig. 1 shows neutron yield from electrons incident on lead [Ref. 5]. The neutron yield increases with the thickness of the lead. With a radiation length of only 5.6 mm, it is clear to see the increase in neutron production for a thick lead piece, 10 cm thick.

For 10 MeV photons, photon attenuation coefficient,  $\mu/\rho$ , in  $\text{cm}^2/\text{g}$  is 2.32E-2 for Al, 2.99E-2 for Fe, 3.10E-2 for Cu, and 4.97E-2 for Pb. Lead is then most effective in attenuating photons; however, as is shown in Fig. 2, ( $\gamma, n$ ) cross-section at 75 MeV for Pb is almost a factor of three higher than Fe. [Ref. 5]; therefore, the superior photon attenuation has associated with it a higher neutron production.

In addition to the direct photon contribution to the dose rate, there is additional photon contribution from ( $n, \gamma$ ) reactions inside these materials.

Secondary photon production leads to the build-up effect which we observed when examining dose rate contributions from neutrons and photons. Figs. 3 and 4 shows this effect in one of the earlier simulations. A similar behavior was observed when the inner lead shielding layer was replaced with carbon steel; although at a lesser magnitude. Fig. 3 shows dose rate attenuation along north-south (Z) and up-down (Y) directions for the lead & normal concrete boxed design. Fig. 4 shows the same distributions for the lead & polyethylene (PE) boxed



*Fig. 1: Neutron yield as a function of electron energy on lead.*

<sup>1</sup> As Quickly As Possible.

design. Details can be found on the e-Linac plone [Ref. 6].

The lead and concrete thicknesses were set to those obtained from the TVLs extracted earlier in order to attenuate photons and neutrons to get to the dose rate levels below the required limits. The Tenth Value Layer (TVL) for photons in lead was found to be 4.3 cm, and for neutrons in concrete, 19 cm, in PE, 7 cm. Using the estimated thicknesses did not reduce the dose rates to below the required levels because of the above-mentioned build-up effect.

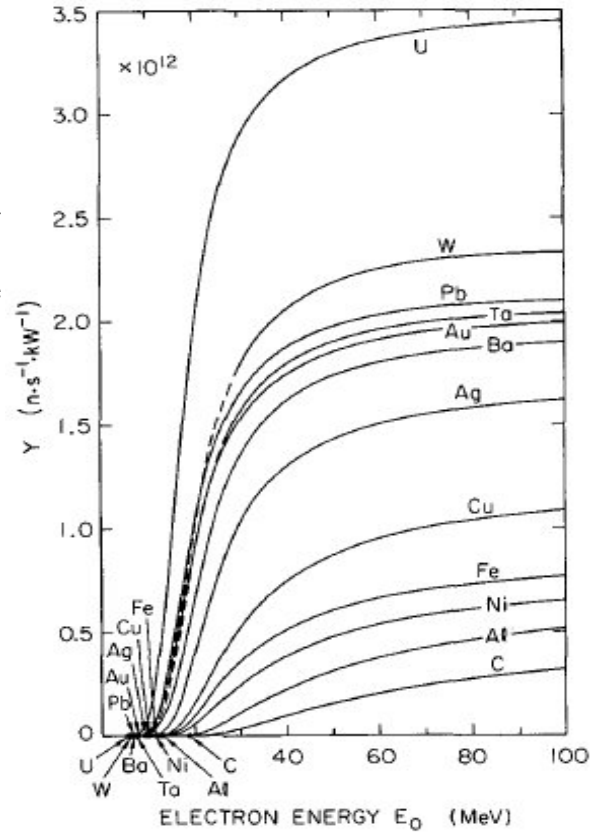


*Fig. 2: Neutron yields from infinitely thick targets, per kW of electron beam power, as a function of electron beam energy  $E_0$ .*

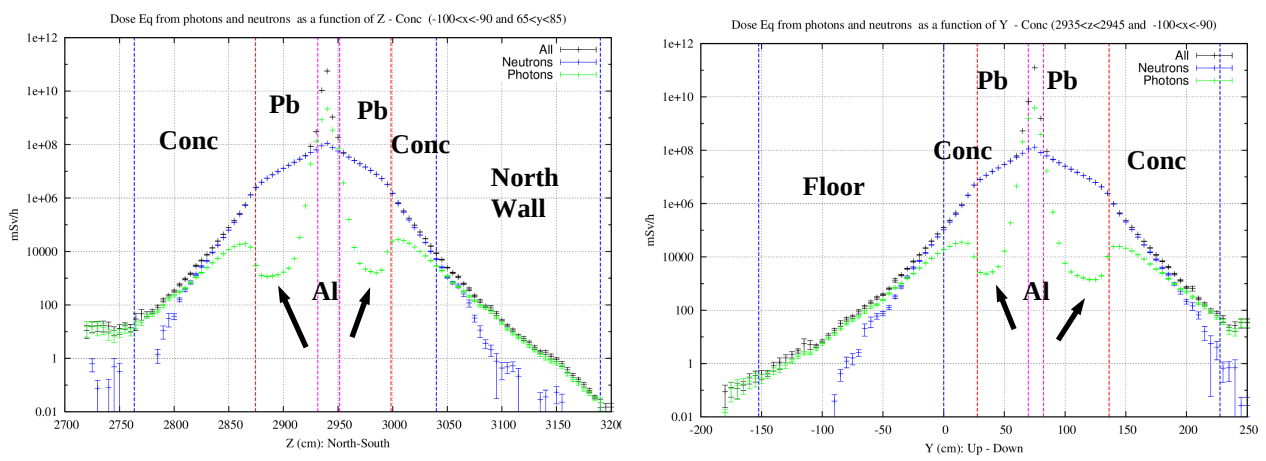


*Fig. 3: Dose rates as a function of Z (left) and Y(right) for the Lead & concrete boxed design.*

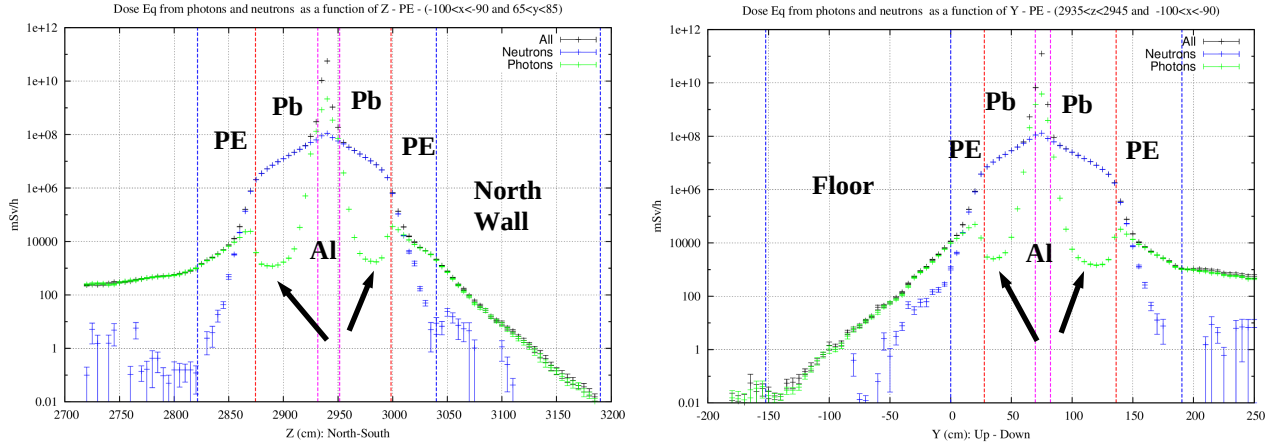


Fig. 4: Dose rates as a function of Z (left) and Y(right) for the lead & PE boxed design.

In order to eliminate the build-up effect observed in the photon fluence (dose rate), two options were considered: 1) a lead, PE sandwich design, 2) lead inner layer around the BD followed by high density concrete (HDC). Layering high and low Z materials to ensure that the gamma and neutron dose rates are each gradually attenuated throughout the thickness of the shielding, proved to be the most efficient configuration.

Table 2: Thicknesses (cm) of Pb, PE, and concrete used in the Pb/PE layering shielding configuration.

Direction	Above	Below	West (0°)	East	North (90°)	South
<b>Pb + PE layers</b>						
<b>Total thickness (cm)</b>	10 Pb	10 Pb	13.5 Pb	10 Pb	10 Pb	10 Pb
	15 PE	15 PE		10 PE	15 PE	15 PE
	10 Pb	10 Pb			10 Pb	10 Pb
	15 PE	15 PE			15 PE	15 PE
	10 Pb	16 Pb			10 Pb	10 Pb
	15 PE				15 PE	15 PE
	47 Conc.				15 Conc.	94 Conc.
<b>High Density concrete</b>						
	10 Pb	10 Pb	13.5 Pb	10 Pb	10 Pb	10 Pb
	139 H.D. Conc.	56 H.D. Conc.		10 PE	80 H.D. Conc.	159 H.D. Conc.

Both of the above solutions worked well, given the thicknesses above in Table 2. Results are shown in Figs 5 and 6. Fig. 5 shows dose rate attenuation along north-south (Z) and up-down (Y) directions for the lead & PE layered design. The order of the Pb, PE, and concrete layers around the BD region (shown B/N magenta lines) are the same as shown in Table 2. Fig. 6 shows the same distributions for the lead & HDC boxed design. Details can be found on the e-Linac plone [Ref. 6].

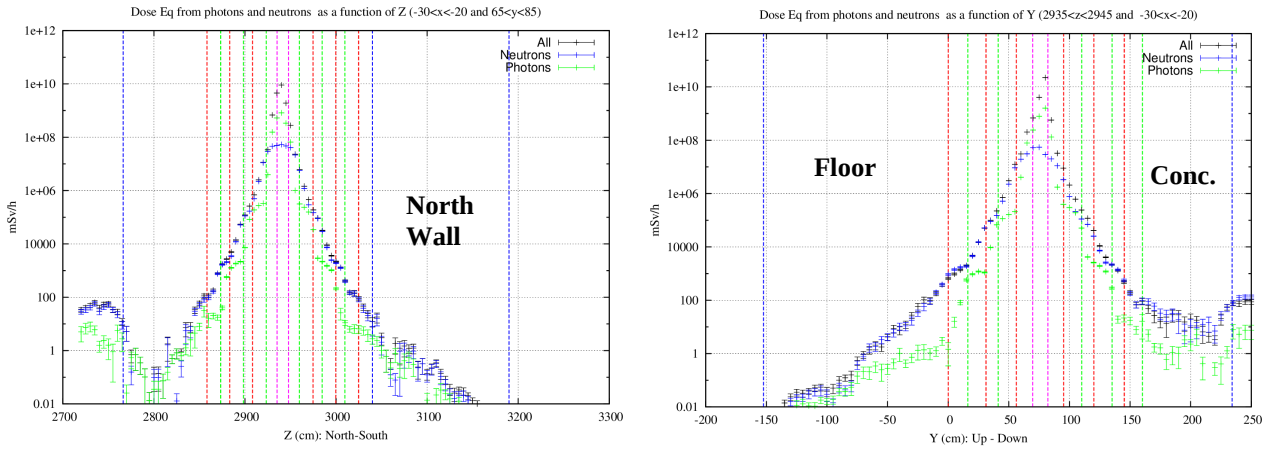


Fig. 5: Dose rates as a function of Z (left) and Y(right) for the lead & PE layered design

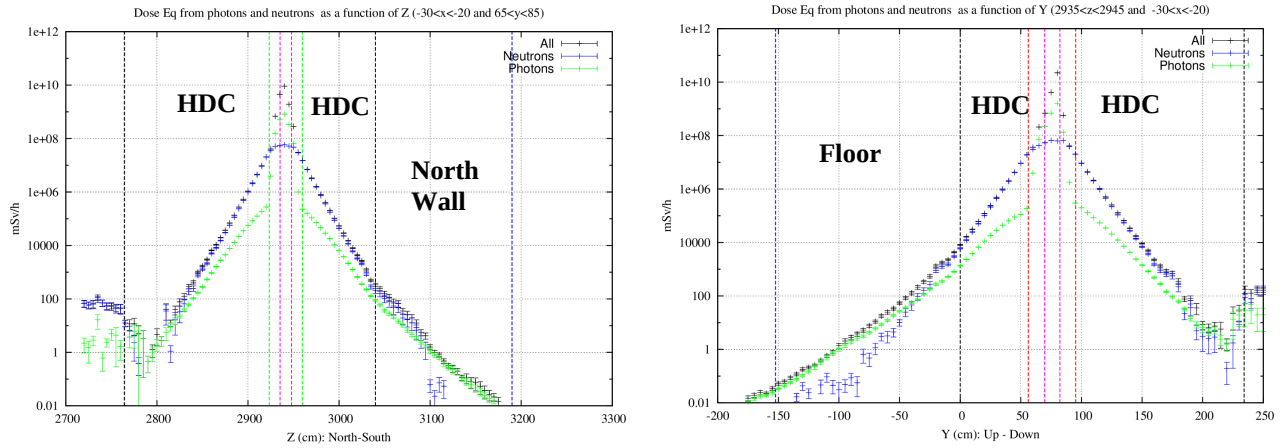


Fig. 6: Dose rates as a function of Z (left) and Y(right) for the lead & HDC boxed design.

Although the above configurations satisfied the dose rate limits, use of both PE and HDC were ruled out. Conventionally, PE is used to slow neutrons down to thermal energies and the addition of boron improves the capture of neutron. PE is more effective at shielding neutrons than concrete but since it is less dense than concrete, it is not as effective at attenuating photons as concrete. The main reason for ruling out PE was the concern over its embrittlement and deterioration of mechanical properties under the high radiation levels for long term operation. A conservative radiation damage threshold for polyethylene is 1E5 Gy [Ref. 7]. The innermost layer of PE is in radiation fields on the order of 1E7 mSv/h. This gives a life time of 1E5 (Sv) / 1E4 Sv/h or 10 hours. The BD is expected to operate one month per year for 20 years. This amounts to 14400 hours of operation. Only the outer PE layers satisfy the dose rate limit of 7 Sv/h (1E5 Sv/14400 h).

HDC attenuates photons because of its high density (around 4 g/cc depending on the composition). It attenuates neutrons through moderation, then capture. High energy neutrons are moderated through inelastic interactions and low energy neutrons through scattering off Hydrogen. Since both processes happen in the same material, HDC is not as effective as having a slab of iron for shielding high energy

neutrons, followed by a hydrogenated material such as PE for low energy neutrons.<sup>2</sup> Other reasons for ruling out HDC were cost, non-uniformity, and unknown composition (unless tested ahead of the time). Considering the above, we decided to go with the following design:

1- An inner layer of lead around the BD, 10 cm thick on the sides and 13.5 cm thick immediately downstream of the BD. The underlying rationale is to reduce photon rates incident on the west wall so as to prevent neutron activation of the second piece of concrete behind the west concrete wall and any interstitial ground water between the two. The BD location is constrained by the beam optics upstream and the space behind the BD is constrained by the position of the West wall. Using steel instead of lead did not achieve the required dose rates at the face of the second concrete piece. The option of drilling a hole behind the BD to insert a 15 cm thick piece of steel was considered but rejected because of the amount of civil work entailed. Also, having stainless steel cooling water piping through cast lead is easier than through steel.

2- The layering configuration was kept because of its efficiency in reducing the dose rates, resulting in smaller bulk shielding.

3- The materials for the layered option were ASTM A36 steel and concrete. In the simulation, the standard FLUKA description of Portland concrete (density of 2.3 g/cc) was modified to include trace amounts of Eu (0.67 ppm), Co (5.2 ppm), and Cs (0.9 ppm), for long term activation in the concrete. These trace amounts were taken from the recently tested sample of concrete used in the UoS TR24 cyclotron. The testing was performed by SRC (Saskatchewan Research Council) using ICP-OES (Inductively Coupled Plasma-Optical Emission Spectroscopy). Carroll and Ramsey [Ref. 8] state concentrations of Eu and Co averaged over the earth's crust are 2.1 ppm and 29 ppm respectively. Other measurements have reported Eu (Co) concentrations of 0.8 (10) ppm. In reality, there is a wide range of values in concentration of the above elements in the concrete sample used, depending on the source and kind of the aggregate in the mix and without testing actual samples that will be used for the shielding, it is not possible to know the exact amount. Regardless, the activation results can be scaled by the ratio of the compositions if testing of the concrete sample is performed at some later point.

4- Two segmentation schemes were investigated: In the initial studies, a Russian doll design was used for the steel and concrete pieces surrounding the innermost lead layer. However, considering ease of construction, another segmentation design was chosen with horizontal slabs in the center and vertical slabs on the sides.

Simulation results presented in this report are for the above material and configuration (aka the final design). For results of other studies, the reader is referred to [Ref. 6].

---

<sup>2</sup> Communications with Alberto Fasso.

# Geometry & beam setup in FLUKA

## Beam Dump Parameters

The tuning beam dump is located in the NW corner of the e-Hall (B2 level). It is made up of Aluminum alloy 6061-T6 and has a rectangular shape with outer dimensions of 134 cm L x 12.6 cm W x 16.9 cm H. The incident plate is at 3.06° with respect to the horizontal plane. This is to spread the heat deposition. The front face of the Beam Dump is 149.9 cm from the West wall. Center of the beam dump is 76 cm above the floor and 98.5 cm from the North wall.

## Beam Specifications

In the initial studies both 100 kW electron beam configurations were considered: 1) 75 MeV, 1.3333 mA (8.114E15 e/s) and 2) 25 MeV, 4 mA (2.4966E15 e/s). Since the high energy results in higher prompt radiation, we used this beam energy and intensity for the remainder of the studies. A rastered beam will be generated by two raster magnets, with center positioned approximately 2 meters upstream of the BD. At the entrance to the BD ( $X = -131.5$  cm), beam shape and size is 4x4 cm square. In the simulation, beam shape was set to a 4x4 cm flat square distribution.

Beam starting position was set upstream of the BD ( $X = -260$  cm)

Beam center is at  $y = 76$  cm from the floor and  $z = 98.5$  cm from the north wall.

Beam starting position was set to  $X = -135$  cm from the west wall.

## Coordinate System Definition

+X: pointing west, with est wall at  $X = 0$  cm.

+Z: pointing north, with north wall at  $Z = 3040$  cm.

+Y: pointing up, with floor at  $Y = 0$ .

## Wall Thicknesses

**North wall:** 150 cm.

**West wall:** 122 cm. There is an additional 208 cm concrete section (540 cm in Z) extending from the floor to  $Y = 330$  cm directly behind the west wall.

**Ceiling:** 183 cm directly above the BD. There is a hatch (604.5 cm in north-south direction, and 275.2cm in east-west direction) above the beam dump for moving large components into and out of the e-Hall.

Fig. 7 shows the plan, side, and beam's eye views of the BD for a slice at the middle of the BD in Y and Z respectively. Shown are the Beam Dump body in magenta, cooling water in blue, air spaces in green, vacuum region in white. The lead layer surrounding the BD (10 cm in the transverse direction and 13.5 cm in the back) is shown in gray.

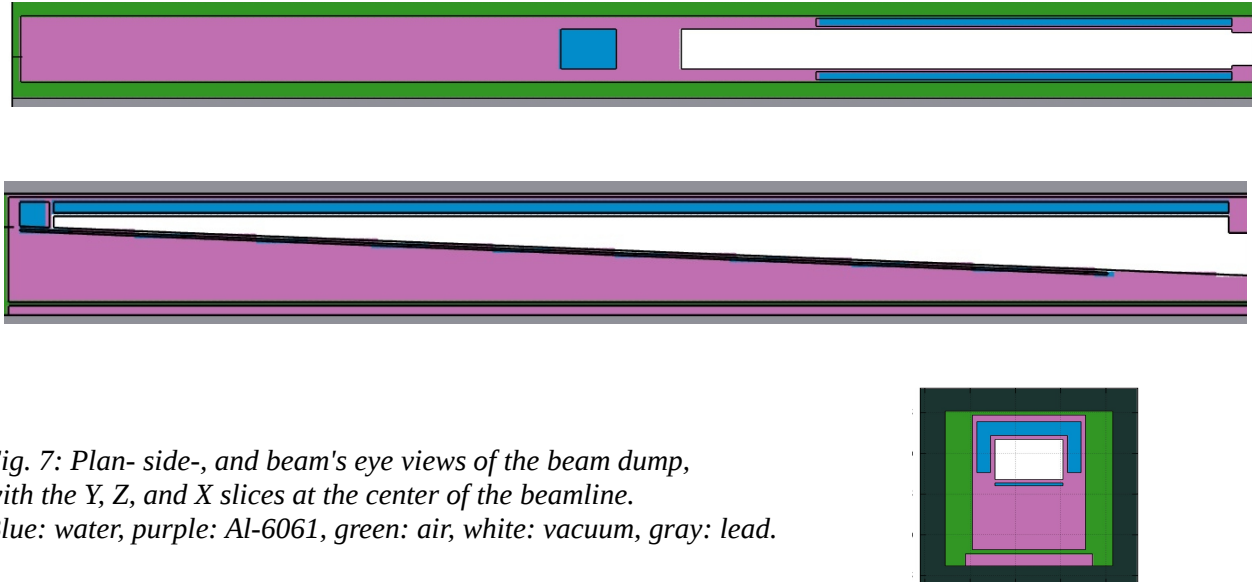
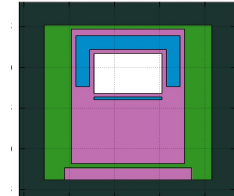


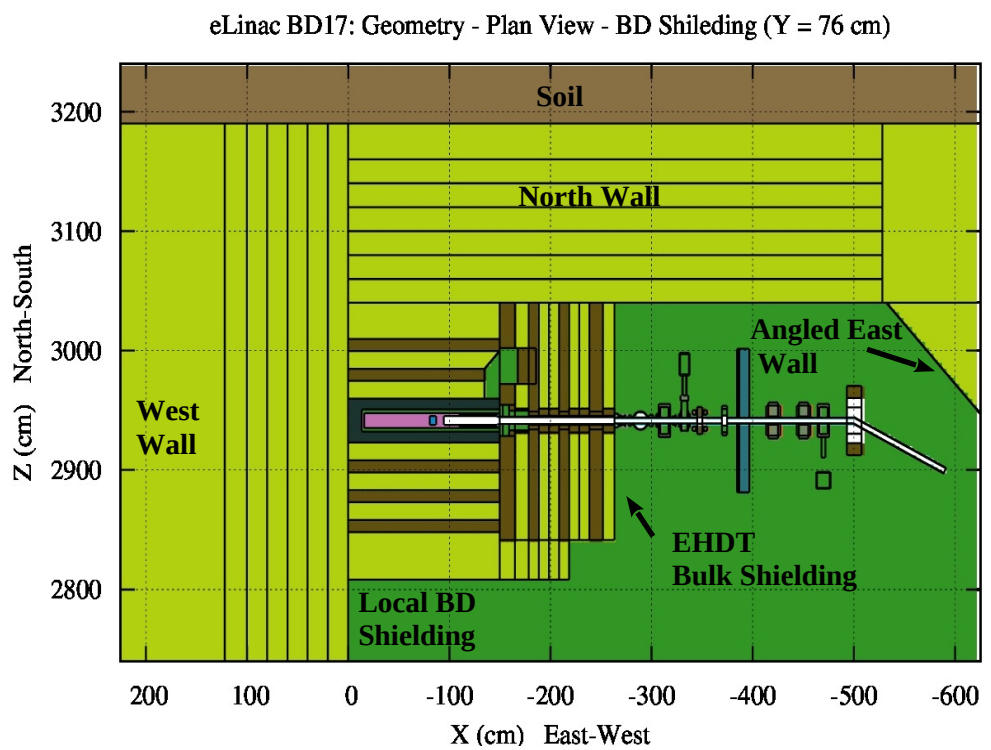
*Fig. 7: Plan- side-, and beam's eye views of the beam dump, with the Y, Z, and X slices at the center of the beamline.*  
*Blue: water, purple: Al-6061, green: air, white: vacuum, gray: lead.*



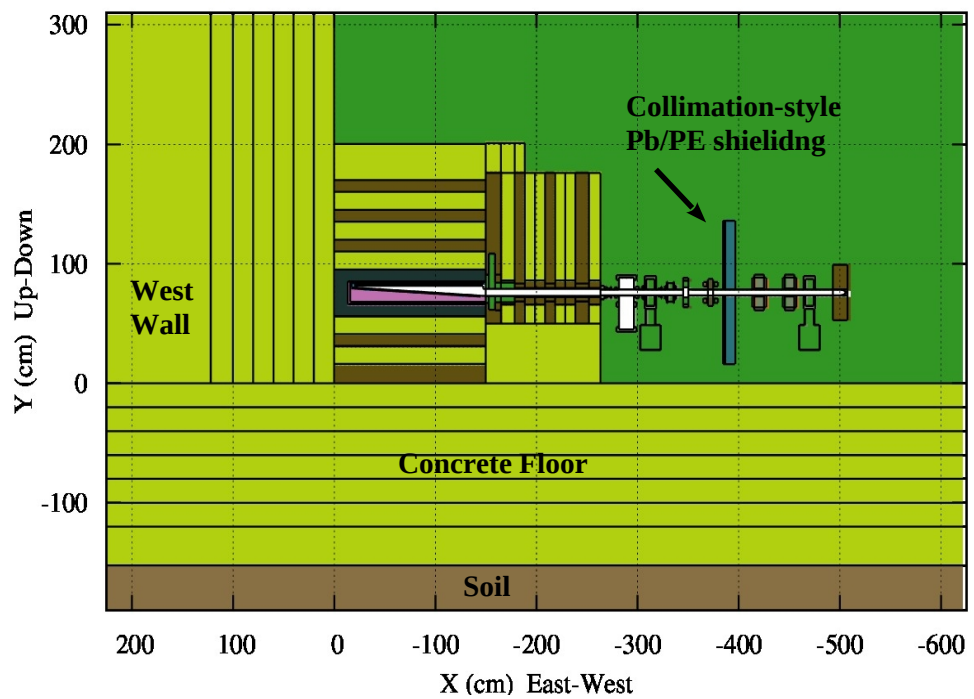
Figs 8-10 shows the top, side, and beam's eye view of the local shielding surrounding the BD. Shown are concrete part of the shielding and concrete walls in yellow, steel shielding in dark brown, soil behind the north wall and the concrete floor in a lighter shade of brown.

*Fig. 8: Top view of the geometry showing North and West walls, the local shielding around the beam dump, the EHDT bulk shielding, the Pb/PE collimation-style shielding, and some of the EHDT beamline components modeled into the simulation.*

*Light brown: soil, yellow: concrete, dark brown: A36 steel, gray: lead, white: vacuum.*



eLinac BD17: Geometry - Side View - BD Shielding ( $Z = 98.5$  cm from the N Wall)



eLinac BD17: Geometry - Beams Eye View ( $X = -90$  cm from the W Wall)

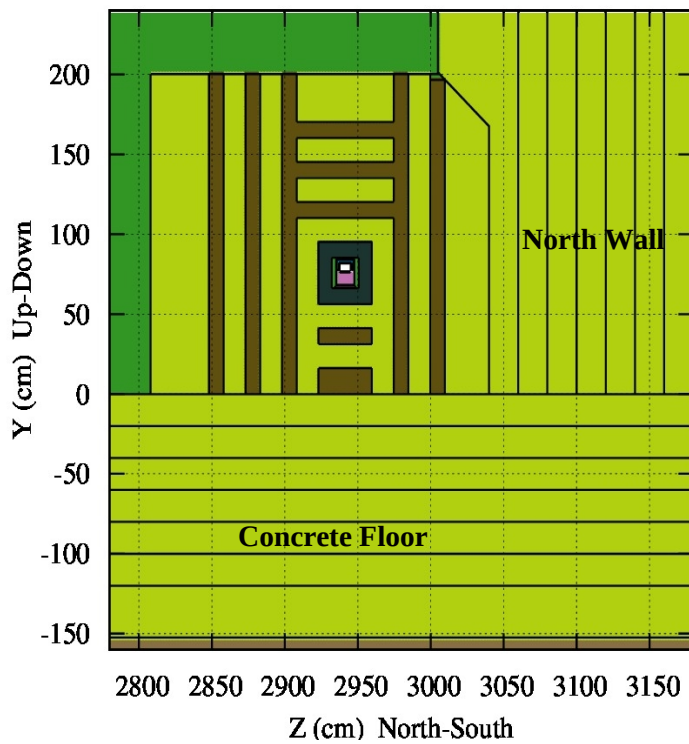


Fig. 9: Side view of the geometry.

Fig. 10: Beam's eye-view of the geometry at the middle of the BD, showing the shielding segmentation arrangement around the beam dump.

## BD Local Shielding Specifications:

Table 3 shows the dimensions of the lead, steel and concrete used in the local shielding for the above final configuration. Outer dimensions of the local shielding are 231.75 in North-South (Z) direction, 161.5 in East-West (X) direction, and 200.2 cm in the Up-Down (Y) direction. This configuration satisfies the dose rate requirements in Table 1.

*Table 3: Local shielding dimensions. The East column contains thicknesses of the upstream bulk shielding.*

Direction	Middle section		Sides			
	Above (90 °)	Below	North (90°)	South	West (0°)	East
Thickness (cm)	10 lead	10 lead	10 lead	10 lead	13.5 lead	0 lead
	15 conc 10 steel 15 conc 10 steel 15 conc 10 steel 30 conc	15 conc 10 steel 15 conc 16.2 steel	15 conc 10 steel 15 conc 10 steel 30.25 conc	15 conc 10 steel 15 conc 10 steel 15 conc 10 steel 40 conc		15 steel 13.6 conc 10 steel 20 conc 10 steel 20 conc 13 steel 11.7 conc
Total (cm)	10 lead 75 conc 30 steel	10 lead 30 conc 26 steel	10 lead 60 conc 20 steel	10 lead 85 conc 30 steel	13.5 lead	0 lead 65 conc 48 steel

## EHDT Shielding Specifications:

The upstream part of the shielding consists of a bulk shielding section and close-in shielding pieces along the beamline to protect the upstream beamline components from the backscattered particles (dominated by photons and neutrons). The bulk part of the EHDT shielding sits on top of a 50 cm high concrete block for support. The EHDT bulk shielding extends:

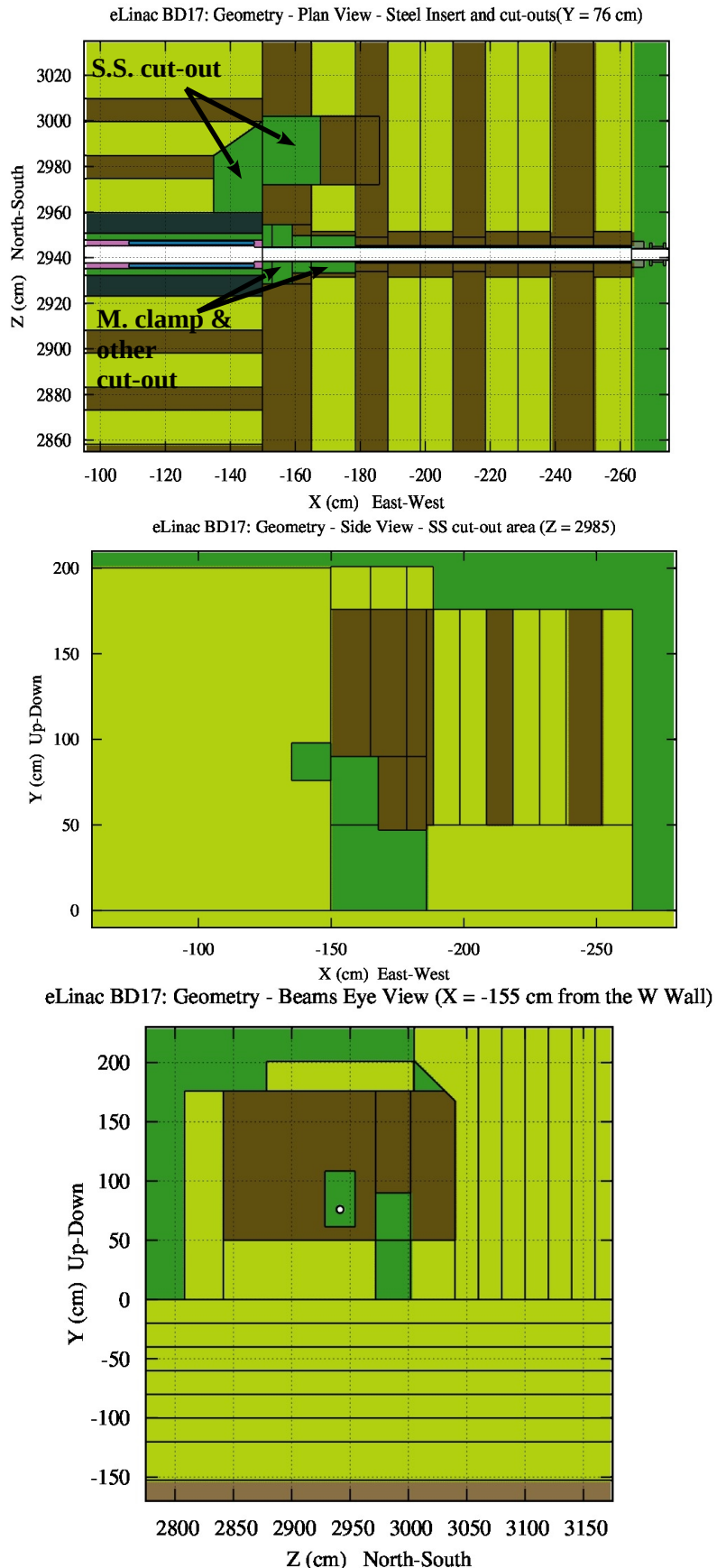
- to the East 113.60 cm from the front face of the BD,
- in the vertical direction, from 50 cm to Beam\_Y + 100 cm ( $Y = 76 + 100 = 176$  cm),
- from the North wall to South, 100 cm from Beam\_Z ( $Z = 2941.5 - 100 = 2841.5$  cm).

Where Beam\_Y and Beam\_Z are the center of the beam axis in the Y and Z directions respectively.

Two additional concrete blocks are placed at the interface of the BD and EHDT bulk she idling, one on the top of the EHDT shielding ( $\Delta X = 40$  cm,  $\Delta Y = 25$  cm,  $\Delta Z = 126$  cm), and one on the side of the EHDT bulk shielding ( $DX = 70$  cm,  $DY = 176$  cm,  $DZ = 25$  cm). This is to prevent the shine from the gaps between the interface of the two shielding.

Several cut-outs were modeled inside the EHDT bulk shielding to accommodate the Marman clamp, water pipes and connections of the service stand (S.S.), and other components immediately upstream of the BD. Two void areas above the Marman clamp and the S.S. were filled with two A36 steel plugs. Fig. 11 shows the top, side, and beam's eye view of the cut-outs and the S.S. plug. The Marman clamp plug is part of one of the EHDT steel plates and not modeled as a separate piece.

*Figure 11: Plan, side, and beam's eye views of the geometry showing the Marman clamp and Service Stand cut-out regions, the S.S. A36 plug, and the A36 insert inside the EHDT bulk shielding, around the beam pipe.*



The A36 steel insert around the beam pipe shown in Fig. 11, inside the EHDT shielding, is an engineering design constraints. The steel and concrete plates need to be modular so that they could be lifted up via the 56 Ton crane through the hatch above. Because of this constraint, an inner steel insert was proposed and modeled into the simulation. Studies showed this feature results in a slight (~3%) increase in the total dose rate upstream of the beam dump, near the beam pipe.

Additional shielding upstream of the EHDT bulk shielding is required to protect the upstream EHDT beamline components and future beamline components, electronics, and equipment to the south of the beamline for future phases of the ARIEL project. A few investigations showed that a combination of a 1" thick lead and 4" thick Polyethylene slabs around the beam pipe is sufficient for protecting the upstream beamline components. See [e-Linac\\_EHDT\\_Shielding\\_18Mar2014.pdf](#) under [Ref. 6].

The closest place this collimation-style shielding could be placed to the EHDT is just downstream of the EHDT Q6, at 390.35 cm from the West wall. The transverse dimensions are:

$$\Delta Y = 176 \text{ cm} \text{ (above the floor)}$$

$$\Delta Z = 120 \text{ cm} \text{ (centered around the beam axis)}$$

In order to extend the lifetime of the PE slab, it is recommended that the 1" lead pipe be placed around the beam pipe, inside the PE.

For the second phase of ARIEL, a wall made up of the same thicknesses of Pb and PE is necessary on the South side to bring dose rates down to the required limit of 1 mSv/h, 3 meters from the beam line close-up views of the collimation-style shielding and the wall.

Figs. 12 and 13 show the top and side views of the EHDT shielding (Wall on the south side and collimation-style shielding around the pipe). PE is in blue and Pb is in gray.

*Fig. 12: Top view of upstream of the EHDT bulk shielding, showing the Pb/PE collimation-style shielding plus the Pb/PE wall on the south side.*

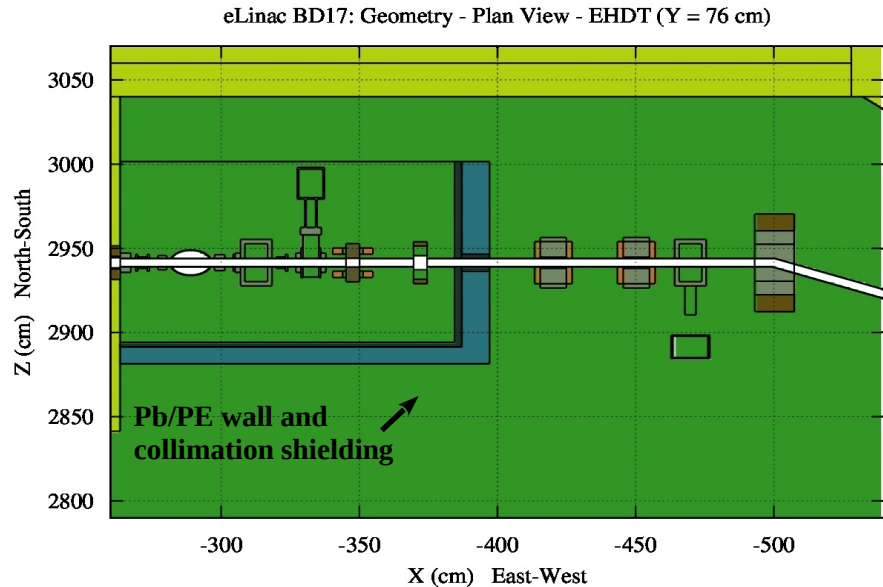
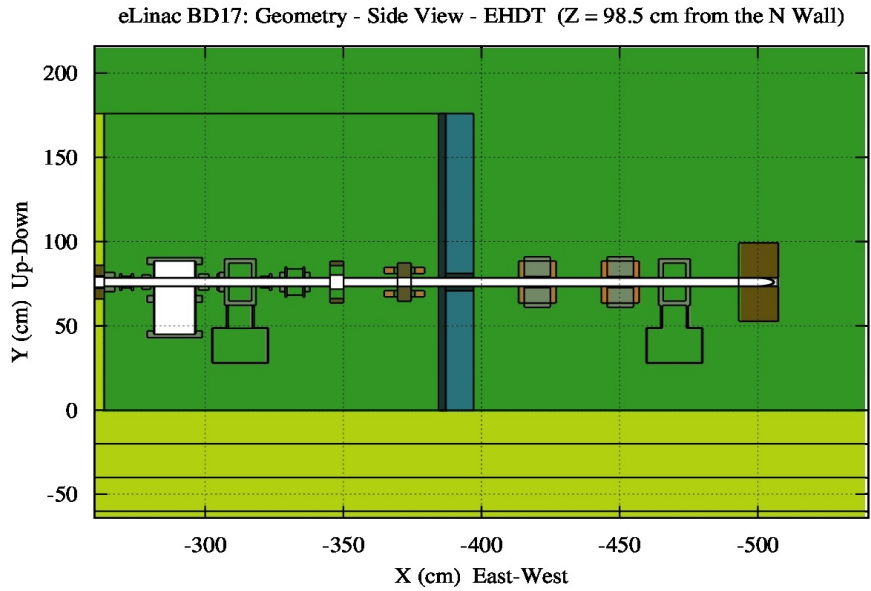


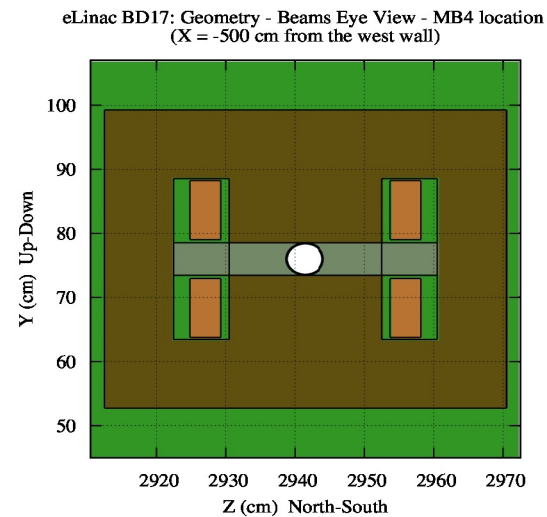
*Fig. 13: Side view of upstream of the EHDT bulk shielding, showing the Pb/PE collimation-style shielding (slice around the beamline).*



Constant magnetic fields were modeled inside the vertical (RMV) and horizontal (RMH) raster magnets with the magnitude of the field set to 0.027 T. Magnetic field of the MB4 Y30 magnet was also modeled with the magnetic field set to 0.74 T in the vertical direction. It was proposed to fill the vacuum box of MB4 with stainless steel to get the backscattered electrons inside the beam pipe to shower in the steel and for attenuating the backscattered photons inside the beam pipe and the generated photons in the shower. This proved to be effective in reducing the dose rates in the concrete wall on the East side. A beam's eye view of the MB4 is shown in Fig. 14. The magnetic field region is constrained to the region between the poles.

The orange region represents the copper coils, the brown region represents the yoke and the poles, the gray region represents the vacuum box filled with stainless steel and the white region is the vacuum inside the beam pipe.

*Fig. 14: Beam's eye view of the MB4 Y30 magnet..  
Orange: Copper coils,  
Gray: stainless steel,  
White: vacuum,  
Brown: A36 steel yoke and poles.*



The last component of the EHDT shielding has to do with the angled wall on the East side. This was to answer the question whether the hole would clean up the back-shine from the back-scattered particles incident on the wall. Several scenarios were investigated to answer the question and to determine the optimum size for the hole. Results showed that coring a hole with a radius of 5 cm and a length (long edge of the cylinder) of 40 cm reduced the back-shine; therefore, reducing the radiation fields from stopping the particles in the wall.

One of the beamline components modeled in the simulation was the CCD camera housed in DB4, placed downstream of MB4. The camera is enclosed in a local shielding box, made up of an inner layer of lead, 1" thick and an outer layer of PE, 3" thick. Fig. 15 shows the beam's eye view of the CCD camera box inside the shielding.

*Fig. 15: Beam's eye view of the CCD camera region, showing 1" Pb and 3" PE shielding.*

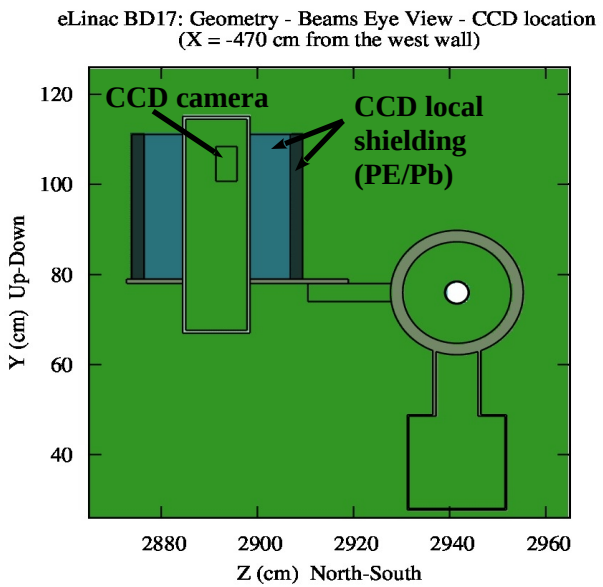


Fig. 16 is the EHDT mechanical drawing, showing the BD insert, the BD local shielding, the upstream bulk shielding and the close-in she idling upstream of the Q6 quadrupole. It also shows beamline components upstream of the BD, some of which were modeled in the simulation.

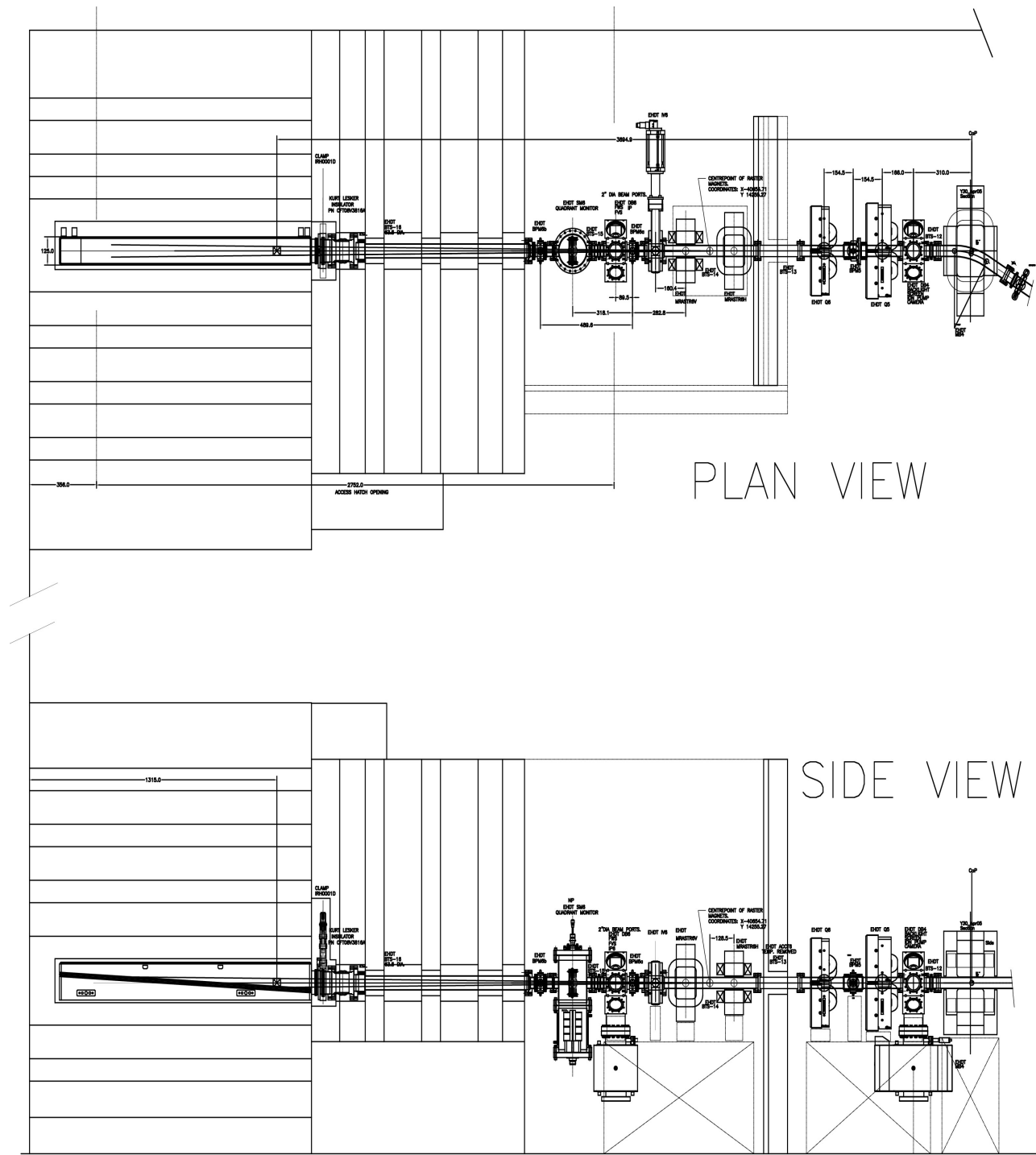
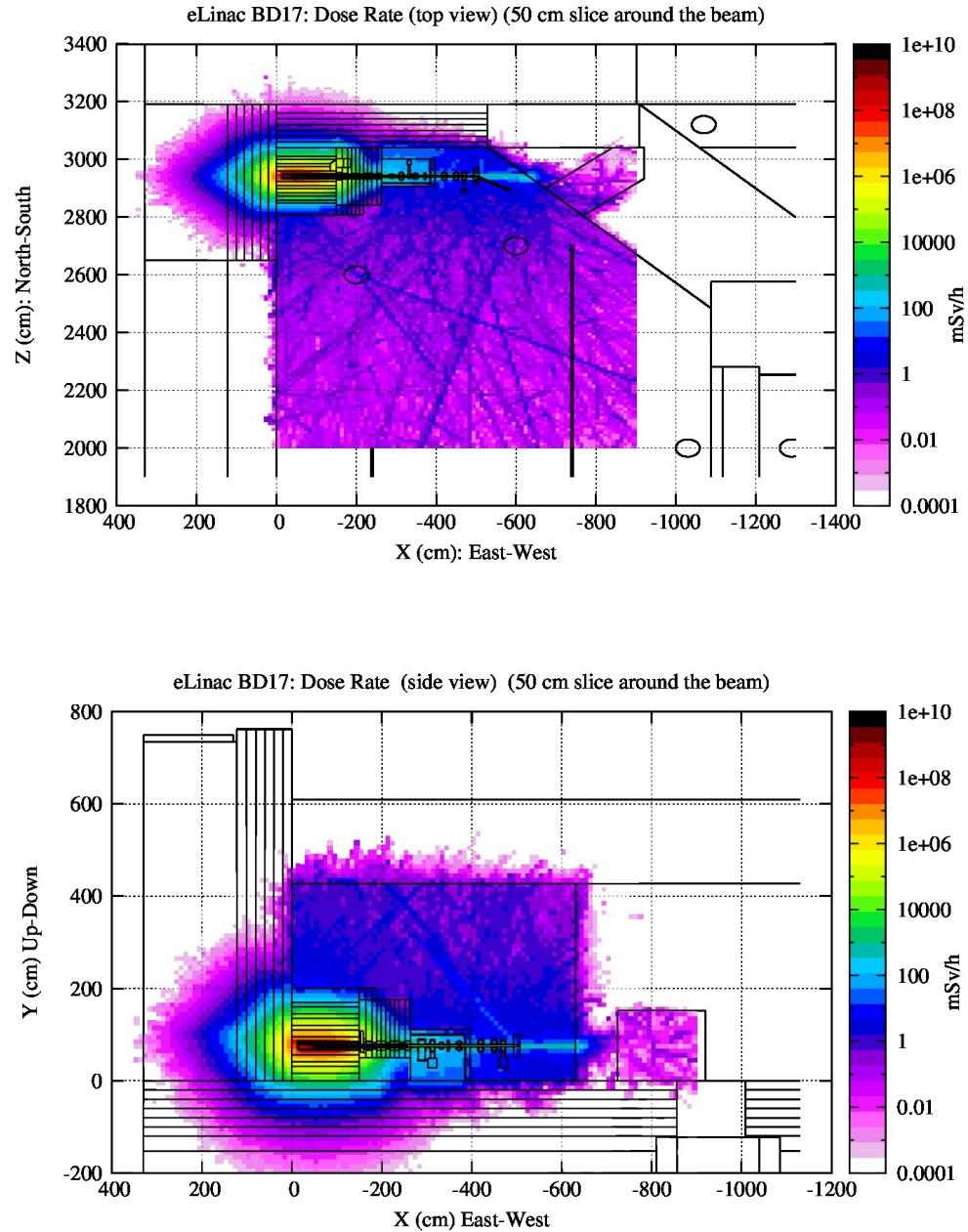


Fig. 16: Mechanical drawing of the EHDT beamline (TEL3749).

## Simulation Results for the Final Local BD Shielding Configuration (lead + steel/concrete)

Results shown for the dose rates around the BD are from the first step part of the simulations. Fig 17 show the plan- and side-view distributions of the total dose rate around the BD. These distributions show an overall view of the radiation fields in and around the BD and the transmission of the radiation through the walls. The results are based on 1.5 B primaries in the first step of the simulation. First step results were used to design the shielding and assess the dose rates around the BD. Second step simulations (discussed later) were used for the design of the EHDT bulk and extra shielding



*Fig. 17: Plan (top) and side (bottom) views of the total dose rate.*

Figure 18 shows the plan view of dose rate distributions with finer binning, to focus on and around the BD.

Contributions from photons, neutrons, and electrons/positrons are shown in the top, middle, and bottom plots respectively.

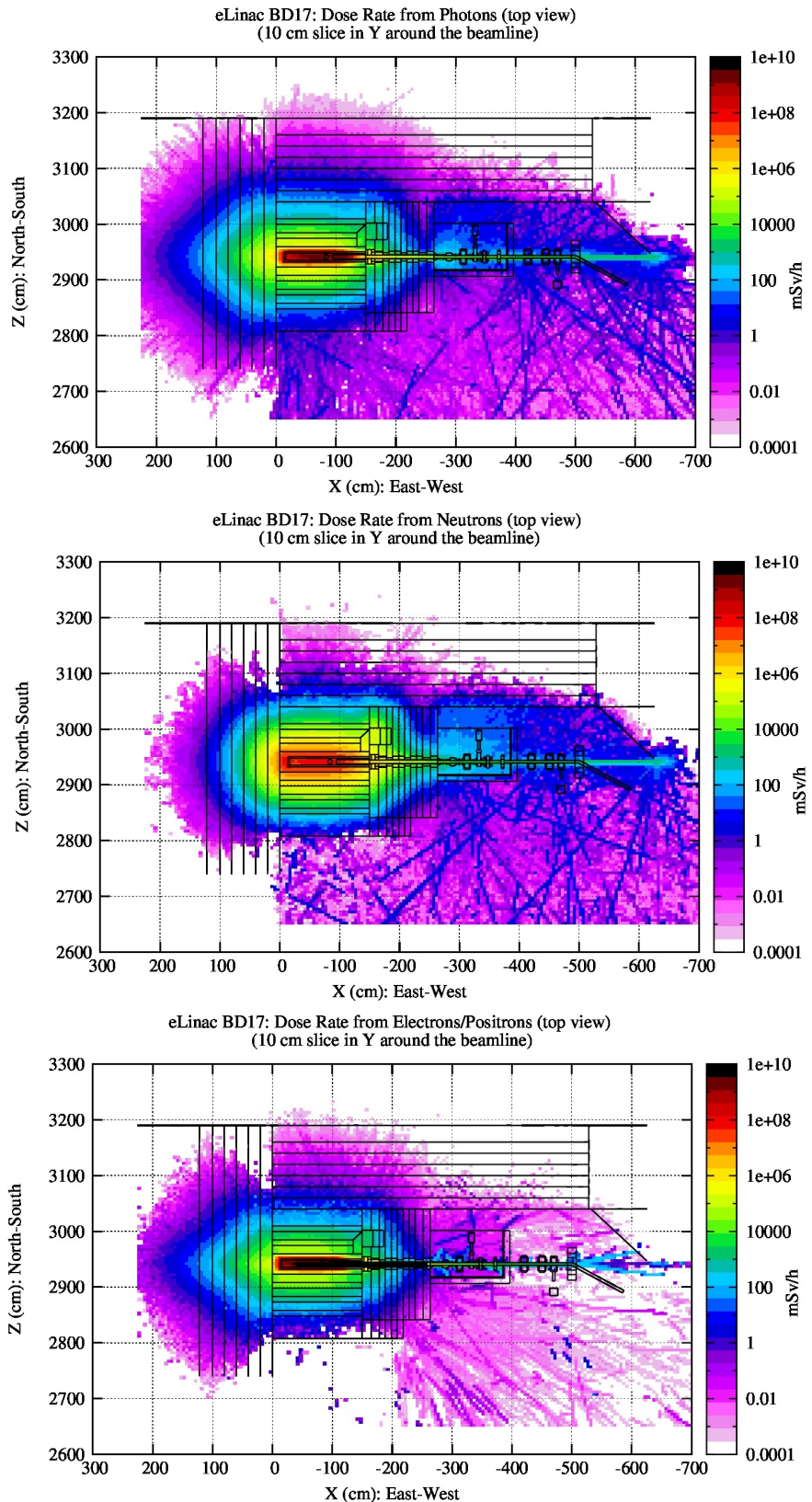


*Fig. 18: Top view of dose rate distributions around the BD. Top: Photons, Middle: Neutrons, Bottom: Electrons & Positrons.*

Figure 19 shows the side view of dose rate distributions with finer binning, to focus on and around the BD.

Contributions from photons, neutrons, and electrons/positrons are shown in the top, middle, and bottom plots respectively.

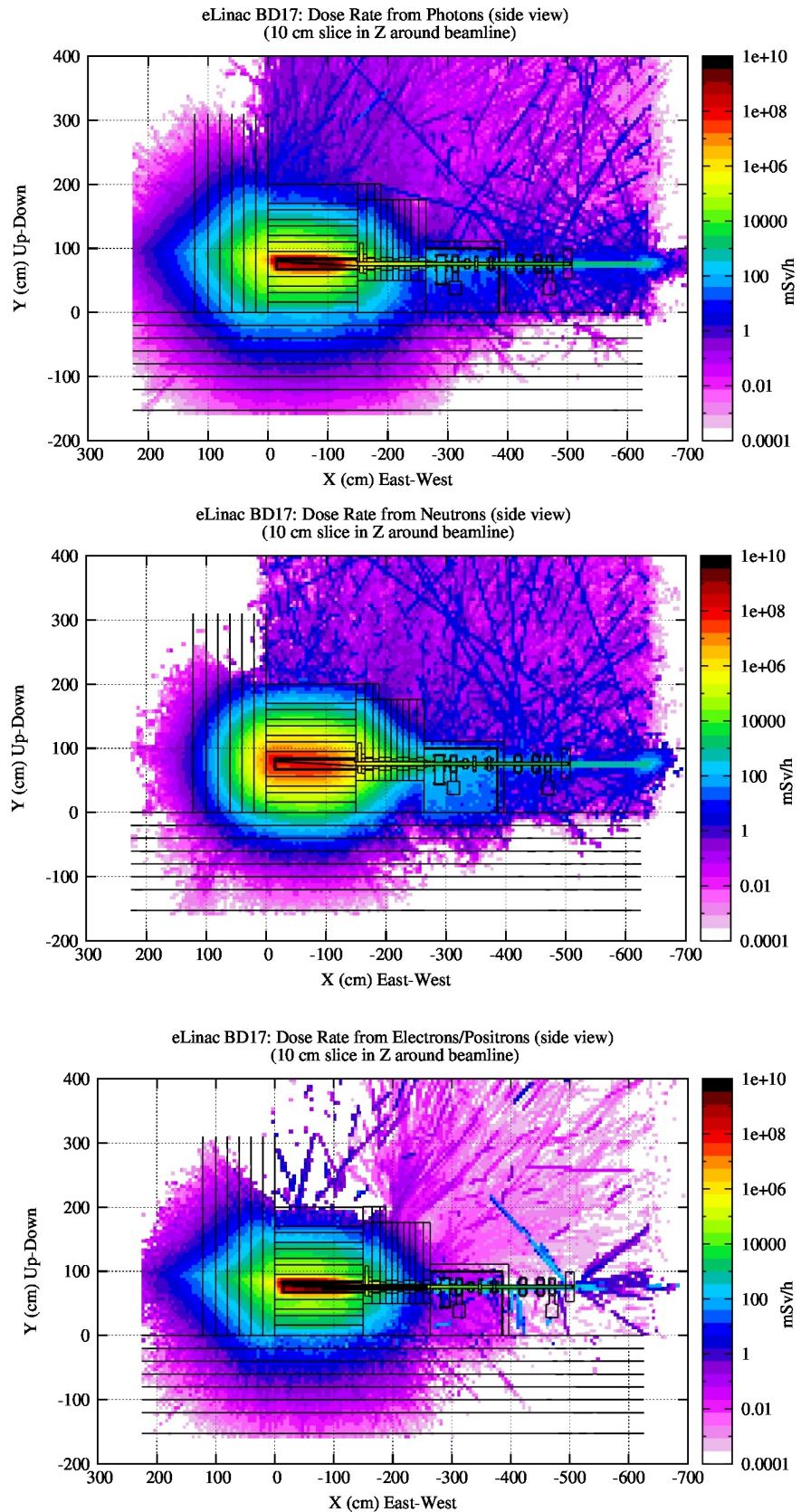


*Fig. 19: Side view of dose rate distributions around the BD. Top: Photons, Middle: Neutrons, Bottom: Electrons & Positrons.*

Figure 20 shows the top and side views of the total dose rate distributions with focus around the BD.

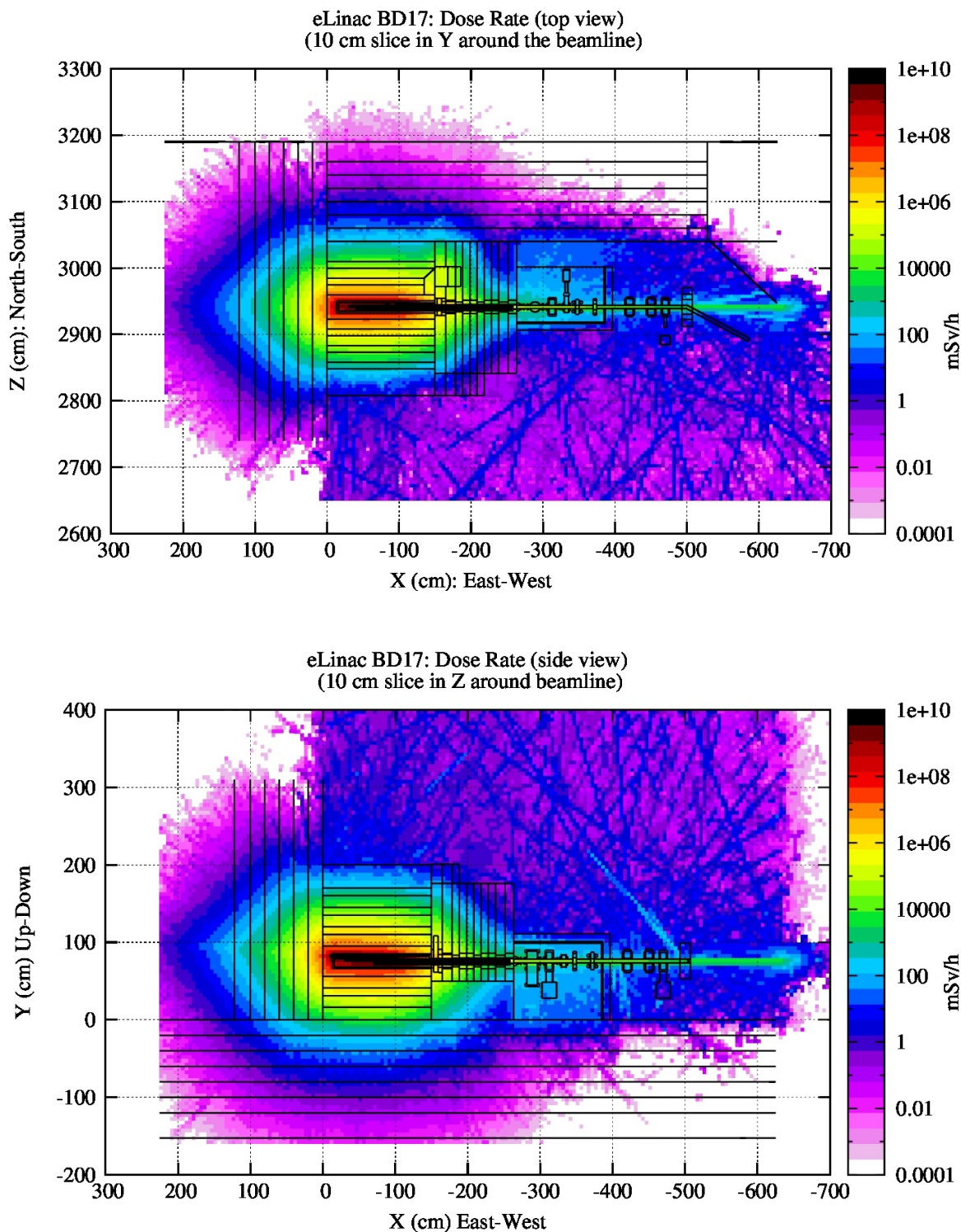


*Fig. 20: Total dose rate distributions. Top: top view, Bottom: side view.*

## Quantitative Values for Dose Rates Outside of the BD Local Shielding

Quantitative values for the dose rates at various boundaries in different directions were obtained by looking at transmission curves. This was obtained from the 1-D projections of the dose rate distributions (shown in Figs. 18-20) as a function of X (East/West), Y(up/down), and Z (North/South). Note that the total dose rate inside the Beam Dump are very high ranging from 1E9 to 1E11 mSv/h or 1 to 100 MSv/h. Total dose rate inside the BD is dominated by contributions from  $e^+$  and  $e^-$ .

Figure 21. shows the dose rate attenuation along the East/West (forward/backward) directions to check the dose rates behind the BD, at the surface of the West wall and at the surface of the soil.

The Z and Y slices are chosen just around the beam pipe since the rates on the West wall is maximum directly behind the BD.

Magenta lines indicate the boundaries of the BD, yellow line shows the extents of the lead shielding behind the BD (same as entrance to the West wall) and the black line indicates the surface of the extra concrete piece behind

the West wall. The thickness of the west wall is 122 cm and the thickness of the the extra concrete behind the West wall is 208 cm. This means the surface of the soil is at X = 330 cm.

Total dose rates at the West wall and the surface of the extra concrete behind the west wall are given in Table 4. Results show that at the soil boundary, the neutron dose rate requirement of 10 mSv/h at the surface of the West wall is not met but this requirement is met at the surface of the concrete piece behind the West wall as well as the soil behind it. This means the section of the West wall directly behind the BD needs to be designated and treated as activated waste at the decommissioning time.

Table 4: Dose rates behind the beam dump.

Contribution	Dose Rates (mSv/h)		
	Surface of West wall	Surface of the extra concrete	Surface of soil (X = 330 cm)
<b>Total</b>	1.3E7	100	< 0.01
<b>Neutrons</b>	1.2 E7	1.4	<< 0.01
<b>Photons</b>	9.0E5	59	
<b><math>e^+e^-</math></b>	1.6E5	36	

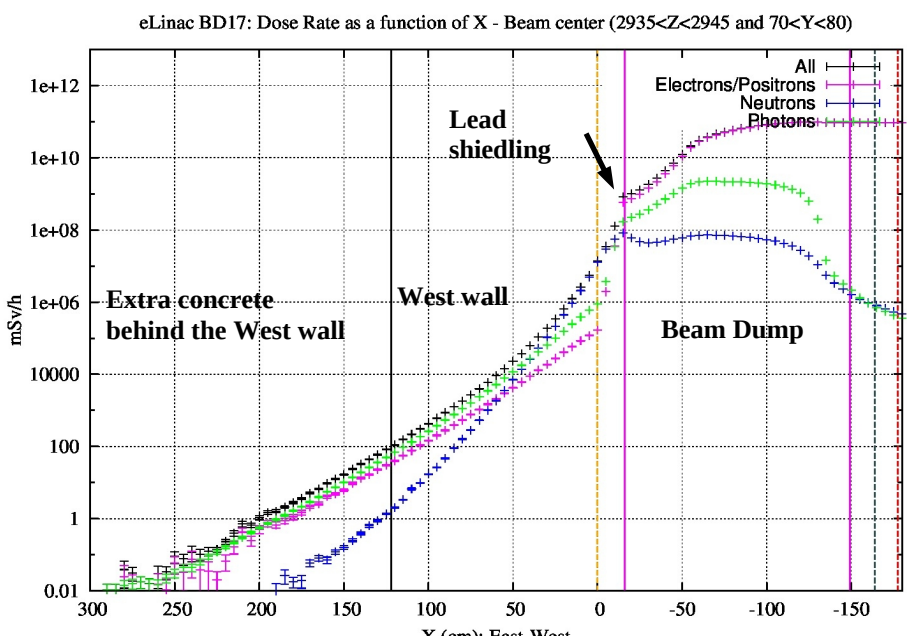
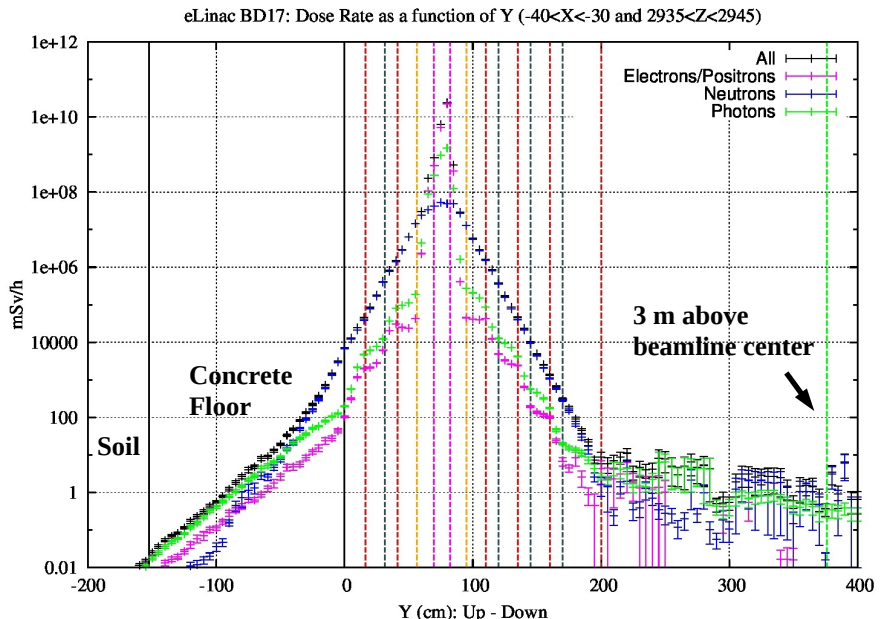


Fig. 21: Dose rate attenuation through the lead and the west concrete wall behind the BD.

To check the dose rates above and below the beam dump we looked at dose rate attenuation through the BD shielding as a function of Y.

Figure 22 shows the transmission curve along the vertical direction. The green line indicates 3 meters above the beamline center. See Table. 3 for thicknesses of the layers.



*Fig. 22: Dose rate distributions as a function of Y (elevation) at the center of the BD.*

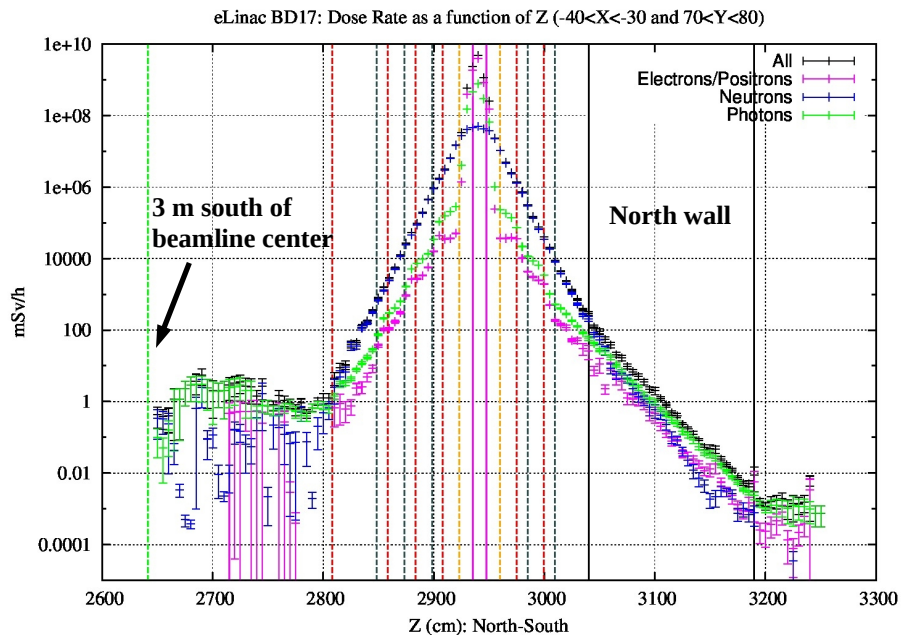
Table 5 shows dose rates above and below the BD (at the center of the BD) at different boundaries. Results show that the dose rate limit of 10 mSv/h from neutrons at the soil level is met. Similarly, the total dose rates just above the BD are below the total 10 mSv/h limit at 3 m.

*Table 5: Dose rates above and below the BD.*

	Dose Rate (mSv/h)	
	Above	
	Outside Surface of the Shielding	Below
<b>Total</b>	~ 11	7012
<b>Neutrons</b>	2.3	6711
<b>Photons</b>	2.8	200
<b>e+/e-</b>	6.0	101

Dose rate limit of 10 mSv/h from neutrons is not met at the surface of the concrete floor but is met at the surface of the soil. This implies the section of the concrete under the BD will be activated above the clearance levels at the end of the operation of the BD and will be designated as activated waste for decommissioning purposes.

To check the dose on the North and South sides of the beam dump we looked at dose rate attenuation through the BD shielding as a function of Z. Figure 23 shows this distribution. The green line on the South sides is at the 3 meter mark from the beamline.



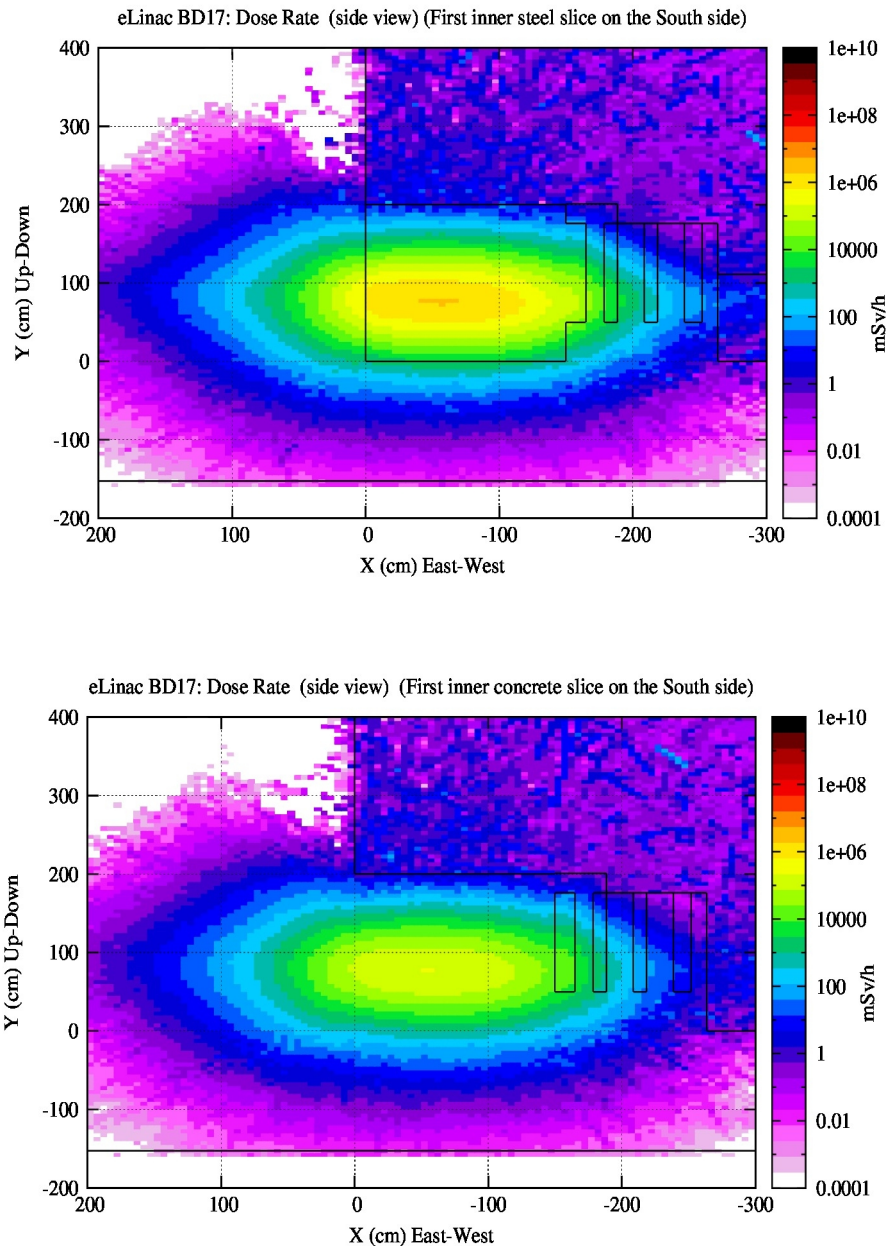
*Fig. 23: Dose rate distributions as a function of Z (North/South) at the center of the BD.*

Table 6 shows dose rates on the sides of the BD at different boundaries. Results show that on the South side, total dose rate limit of 3 mSv/h at 3 m is met. On the North side, at the surface of the concrete wall, neutron dose rate limit of 10 mSv/h is not met; therefore, the concrete directly beside the BD will need to be designated as radioactive waste at decommissioning time. The neutron dose rate limit of 10 mSv/h at the surface of the soil is met.

*Table 6: Dose rates to the North and South of BD.*

	Dose Rate (mSv/h)		
	South	North	
	Outside surface of the shielding	Surface of the concrete wall	Surface of the soil
<b>Total</b>	< 1	~ 313	< 0.01
<b>Neutrons</b>	0.3	207	<< 0.01
<b>Photons</b>	0.1	55	
<b>e+/e-</b>		23	

The question of photon leakage through the concrete part of the shielding and neutron leakage through the steel part of the shielding arose due to the segmentation scheme used in the final configuration. Fig. 24 shows side view distributions of the total dose rate for a slice around the first steel and concrete layers on the south side (steel slice at  $2905 < Z < 2910$  and concrete slice at  $2890 < Z < 2895$ ). No obvious neutron leakage through the steel piece or photon leakage through the concrete piece is observed. Dose rates in the steel layer are higher because it is closer to the BD. Photons and neutrons are coming out at an angle with respect to the vertical axis at the sides of the BD and therefore, go through multiple layers of concrete and steel.



*Fig. 24: Side view of the total dose rate distribution for a slice in the first concrete section on the south side (top) and for a slice in the first steel section on the south side (bottom).*

## Residual Dose Rates

Residual dose rates from the activation of the BD, the BD shielding and the EHDT shielding was investigated. The operational conditions assumed was 100 kW (75 MeV, 1.33333 mA) electron beam incident on the BD one month of the year for 20 years.

Fig. 25 shows top and side views of the residual dose rate distribution, 8 hours after EOB. The requirements ask for residual dose rates of  $\leq 100 \mu\text{Sv}/\text{h}$ , 1 meter south of the outside edge of the EHDT shielding. Results show this requirement is well met where the residual dose rate are around 0.01 mSv/h or  $10 \mu\text{Sv}/\text{h}$ , an order of magnitude less than the requirement.

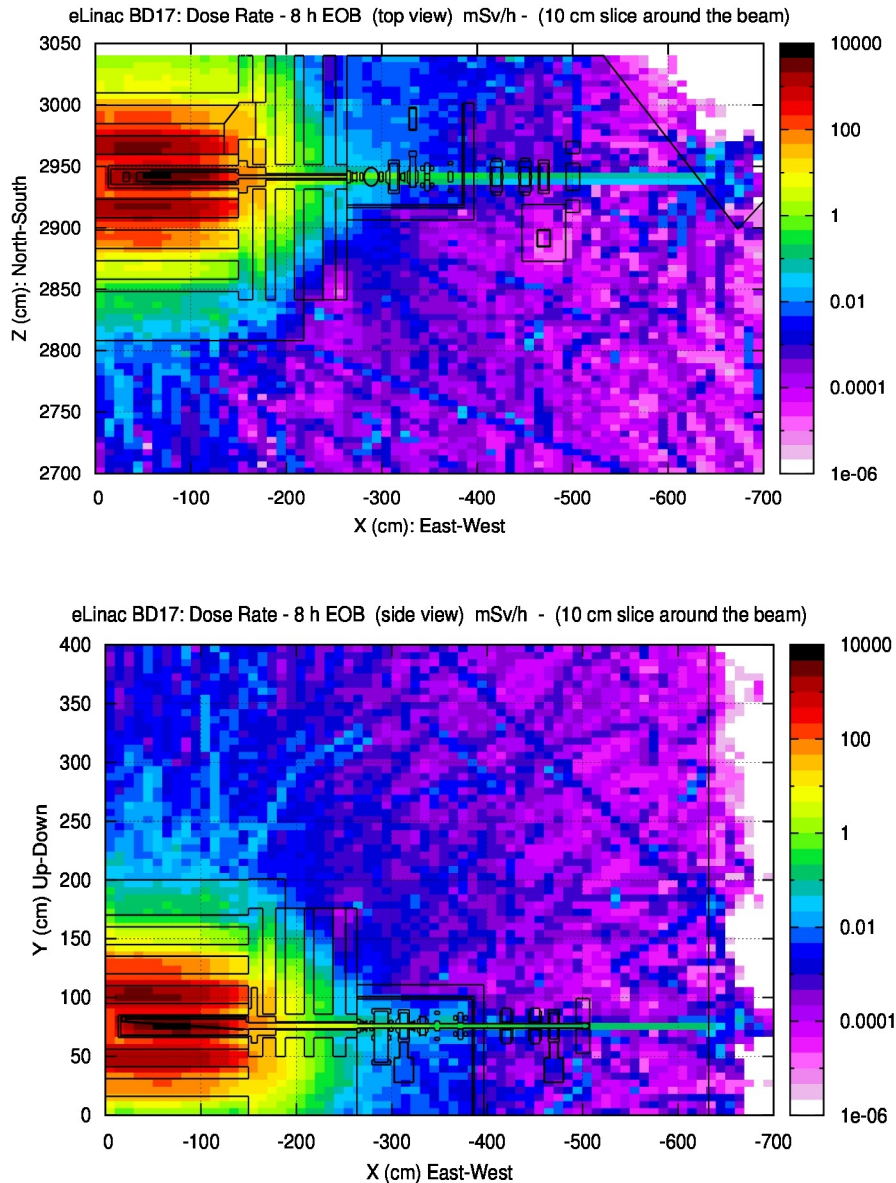
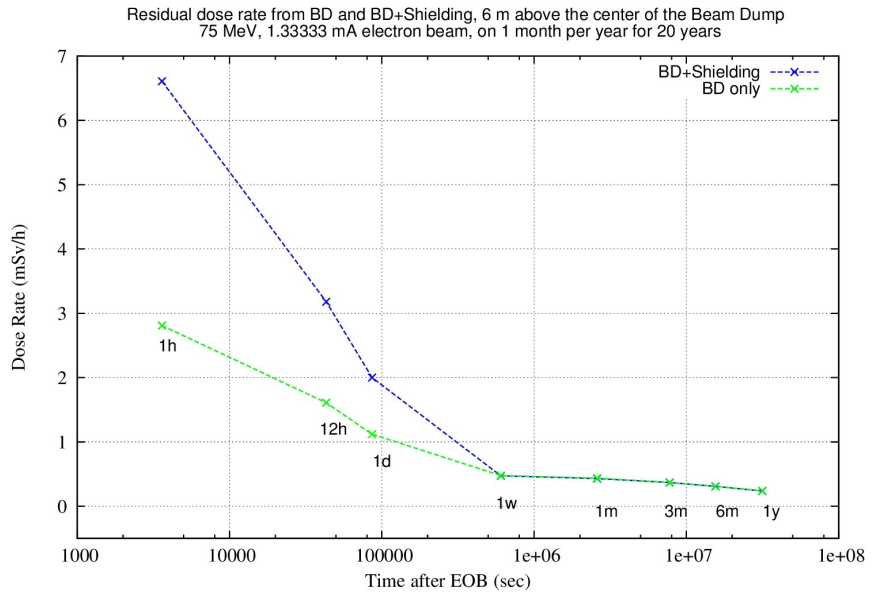


Fig. 25: Residual dose rate distribution, 1 shift (8 hours) after EOB. Top: top view, Bottom: side view.

We also checked residual dose rates above the uncovered BD and the BD local shielding as a function of cooling time. Fig 26 shows residual dose rates, 6 meters above the center of the BD, due to activation of the BD, the BD local shielding components remaining in the eHall and the upstream bulk shielding, as a function of cooling time after end of beam (EOB).

*Table 7: Residual dose rate from BD and BD shielding components.*

Time after EOB	DR (mSv/h)	
	BD	BD + lead + conc/steel
0 s	61.8	66.7
1 h	2.81	6.61
12 h	1.61	3.18
1 d	1.12	2.00
1 w	0.48	0.47
1 m	0.44	0.43
3 m	0.37	0.36
6 m	0.31	0.31
1 y	0.24	0.23



*Fig. 26: Residual dose rate from BD (in green) and BD+shielding (in blue), 6 meters above the center of the BD.*

## Activation Results

Dominant contributions to the residual dose rate, from the activities of the BD, the cooling water, the lead, steel, and concrete components of the Local shielding, can be identified from results of this section. The long-lived activation species driving the decommissioning have been determined.

*Table 8: Production rates and Activation in the beam dump cooling water.*

### Activation in the BD Cooling Water

Table 8 shows production rates of C-11, N-16, N-13, and O-15 in the BD cooling water as well as activities 1 week and 1 month after EOB.

Isotope	Production rate (Nuclei/sec)	Activity (Bq)	
		1 week after EOB	1 month after EOB
H-3	2.61E+10	1.51E+09	1.51E+09
Be-7	1.04E+10	3.10E+09	3.10E+09
C-11	7.33E+10		
N-16	8.29E+08		
N-13	9.74E+09		
O-15	3.63E11		

**Activation in the BD Al 6061:** Activities, 1 week and 1 month after EOB are shown in Table 9. Only isotopes with activities greater than 1E3 Bq are included..

*Table 9: Activation in the beam dump Al 6061.*

Isotope	Activity (Bq)			
	1 day after EOB	1 week after EOB	1 month after EOB	1 year after EOB
H-3	4.02E+09	4.02E+09	4.00E+09	3.80E+09
BE-7	1.09E+06	1.06E+06	7.88E+05	9.59E+03
C-14	1.52E+05	1.53E+05	1.53E+05	1.52E+05
F-18	1.16E+06			
Na-24	2.63E+10	3.32E+07		
Na-22	2.82E+10	2.81E+10	2.76E+10	2.16E+10
Mg-28	3.61E+05	3.17E+03		
Al-28	3.62E+05	3.18E+03		
Al-26	1.34E+07	1.34E+07	1.34E+07	1.34E+07
Si-31	8.05E+05			
Ar-39	1.99E+03	2.59E+03	2.59E+03	1.99E+03
K-42	1.25E+05			
Ca-45	6.12E+05	6.52E+05	5.91E+05	1.31E+05
Sc-48	6.88E+06	6.92E+05		
Sc-47	1.09E+08	3.12E+07	2.66E+05	
Sc-46	3.33E+07	3.24E+07	2.68E+07	1.64E+06
Sc-44	1.08E+07	1.92E+06	1.60E+05	1.55E+05
Sc-43	1.34E+04			
Ti-45	5.77E+05			
Ti-44	1.57E+05	1.58E+05	1.57E+05	1.55E+05
V-49	1.68E+09	1.67E+09	1.59E+09	7.97E+08
V-48	1.30E+09	1.00E+09	3.69E+08	
Cr-51	1.09E+11	9.34E+10	5.25E+10	1.20E+07
Cr-48	3.12E+07	3.05E+05		
Mn-56	1.59E+08			
Mn-54	1.03E+10	1.02E+10	9.69E+09	4.61E+09
Mn-53	1.54E+04	1.54E+04	1.54E+04	1.54E+04
Mn-52	1.02E+09	4.88E+08	2.82E+07	
Fe-59	4.82E+07	4.42E+07	3.09E+07	1.66E+05
Fe-55	3.00E+10	2.98E+10	2.94E+10	2.33E+10
Fe-52	5.27E+06			
Co-61	2.95E+04			
Co-60	4.03E+07	4.02E+07	3.99E+07	3.54E+07
Co-58	1.20E+09	1.14E+09	9.07E+08	3.42E+07

Co-57	7.21E+07	7.09E+07	6.69E+07	2.85E+07
Co-56	1.26E+07	1.23E+07	1.00E+07	4.82E+05
Co-55	1.86E+05			
Ni-66	3.72E+06	5.82E+05		
Ni-65	1.47E+04			
Ni-63	2.69E+07	2.67E+07	2.67E+07	2.67E+07
Ni-59	9.01E+04	9.01E+04	9.01E+04	9.01E+04
Ni-57	1.80E+06	1.26E+05		
Cu-67	6.00E+08	1.18E+08	2.43E+05	
Cu-66	3.72E+06	5.82E+05		
Cu-64	3.40E+10	1.31E+07		
Cu-62	3.18E+08	6.09E+03		
Cu-61	1.10E+08			
Zn-69	5.85E+08	4.16E+05		
Zn-65	5.55E+09	5.46E+09	5.11E+09	1.98E+09
Zn-62	3.13E+08	5.99E+03		
Ga-67	3.88E+05	4.69E+04		

**Activation in the BD Local Lead Shielding:** Activities, 1 week and 1 month after EOB are shown in Table 10. Only isotopes with activities greater than 1E3 Bq are included.

*Table 10: Activation in the beam dump local lead shielding.*

Isotope	Activity (Bq)			
	1 day after EOB	1 week after EOB	1 month after EOB	1 year after EOB
H-3	3.39E+06	3.40E+06	3.38E+06	3.21E+06
BE-7	1.04E+05	1.25E+05	9.29E+04	
C-14	2.43E+04	2.58E+04	2.58E+04	2.43E+04
Sr-92	1.40E+03			
Sr-91	8.02E+04			
Sr-90	6.08E+03	1.22E+03	1.22E+03	5.94E+03
Sr-89	2.71E+05	3.25E+05	2.37E+05	1.84E+03
Y-93	6.18E+04			
Y-92	2.20E+04			
Y-91	1.36E+05	1.07E+05	8.13E+04	1.83E+03
Y-90	6.04E+03			5.94E+03
ZR-95	1.77E+05	2.15E+05	1.68E+05	3.43E+03
Nb-95	5.53E+04	8.87E+04	1.25E+05	7.31E+03
Ru-106	3.61E+04	4.64E+04	4.45E+04	1.84E+04
Ru-105	7.66E+03			

Ru-103	1.31E+05	7.68E+04	5.12E+04	
Rh-106	3.61E+04	4.64E+04	4.45E+04	1.84E+04
Rh-105	2.28E+05	1.77E+04		
Pd-112	1.45E+05			
Pd-111	6.11E+03			
Pd-109	9.52E+04			
Ag-113	1.29E+04			
Ag-112	1.70E+05			
Ag-111	4.14E+05	3.08E+05	3.62E+04	
Pt-193	4.50E+04	4.39E+04	4.39E+04	4.44E+04
Au-195	8.97E+04	1.17E+05	1.08E+05	2.38E+04
Au-193	1.15E+06	3.94E+03		
Hg-203	6.17E+07	5.70E+07	4.05E+07	2.75E+05
Hg-197	1.12E+07	2.57E+06	6.64E+03	
Hg-195	2.01E+05	1.79E+04		
Tl-204	2.26E+08	2.27E+08	2.25E+08	1.89E+08
Tl-202	2.98E+09	2.12E+09	5.78E+08	1.40E+06
Tl-201	9.07E+09	2.38E+09	1.25E+07	
Tl-200	2.41E+09	1.26E+08		
Tl-199	4.64E+07			
Tl-198	5.02E+06			
Tl-197	1.53E+04			
Pb-209	3.65E+08			
Pb-205	5.69E+05	5.69E+05	5.69E+05	5.69E+05
Pb-203	3.40E+11	4.97E+10	3.11E+07	
Pb-202	1.41E+06	1.41E+06	1.41E+06	1.41E+06
Pb-201	1.68E+09	3.81E+04		
Pb-200	1.30E+09	1.25E+07		
Pb-199	5.34E+03			
Bi-207	2.57E+05	2.78E+05	2.78E+05	2.51E+05
Bi-206	7.56E+06	4.22E+06	3.28E+05	
Bi-205	6.16E+06	5.31E+06	1.88E+06	
Bi-204	5.08E+05			
Bi-203	1.55E+05			

**Activation in the BD Local Steel Shielding:** Activities, 1 week and 1 month after EOB are shown in Table 11. Only isotopes with activities greater than 1E3 Bq are included.

*Table 11: Activation in the beam dump local steel shielding.*

Isotope	Activity (Bq)			
	1 day after EOB	1 week after EOB	1 month after EOB	1 year after EOB
H-3	2.84E+05	2.78E+05	2.77E+05	2.69E+05
BE-7	5.21E+04	6.26E+04	4.64E+04	
Si-31	6.30E+05			
P-33	9.51E+05	8.18E+05	4.36E+05	
P-32	6.93E+08	5.24E+08	1.71E+08	
S-35	.36E+07	1.29E+07	1.07E+07	7.61E+05
Sc-48	1.09E+05	1.45E+04		
V-49	4.07E+05	4.03E+05	3.85E+05	1.93E+05
V-48	1.12E+05	1.13E+05	4.15E+04	
Cr-51	8.53E+07	7.19E+07	4.04E+07	9.46E+03
Mn-56	1.78E+09			
Mn-54	7.75E+08	7.64E+08	7.26E+08	3.45E+08
Mn-52	6.04E+06	2.69E+06	1.55E+05	
Fe-59	1.02E+10	9.25E+09	6.47E+09	3.50E+07
Fe-55	9.07E+10	9.03E+10	8.89E+10	7.04E+10
Fe-52	2.14E+04			
Co-60	1.61E+09	1.60E+09	1.59E+09	1.41E+09
Co-58	1.85E+05	1.25E+05	1.00E+05	5.27E+03
Co-56	7.80E+04	9.61E+04	7.82E+04	2.98E+03
Ni-63	4.63E+05	4.60E+05	4.60E+05	4.59E+05
Cu-64	1.25E+10	4.82E+06		

**Activation in the Local Concrete Shielding:** Activities, 1 week and 1 month after EOB are shown in Table 12. Only isotopes with activities greater than 1E3 Bq are included.

*Table 12: Activation in the beam dump local concrete shielding.*

Isotope	Activity (Bq)			
	1 day after EOB	1 week after EOB	1 month after EOB	1 year after EOB
H-3	5.00E+06	5.13E+06	5.11E+06	4.73E+06
BE-7	3.64E+05	3.12E+05	2.31E+05	3.20E+03
C-14	7.76E+03	8.37E+03	8.37E+03	7.76E+03
Na-24	4.42E+11	5.59E+08		
Na-22	5.05E+06	5.11E+06	5.02E+06	3.87E+06
Mg-28	2.17E+05	2.38E+03		
Al-28	2.17E+05	2.38E+03		
P-32	8.19E+05	6.84E+05	2.24E+05	
S-35	6.83E+05	5.79E+05	4.83E+05	3.82E+04
Cl-36	2.86E+04	2.88E+04	2.88E+04	2.86E+04
Ar-39	4.19E+07	4.19E+07	4.19E+07	4.18E+07
Ar-37	7.55E+09	6.73E+09	4.27E+09	5.63E+06
K-43	9.92E+05	1.17E+04		
K-42	3.19E+10	9.96E+06		
K-40	2.13E+03	2.13E+03	2.13E+03	2.13E+03
Ca-47	9.76E+07	3.96E+07	1.18E+06	
Ca-45	1.13E+10	1.10E+10	9.95E+09	2.41E+09
Ca-41	1.74E+07	1.74E+07	1.74E+07	1.74E+07
Sc-47	1.10E+08	7.43E+07	3.84E+06	
Cr-51	3.10E+06	2.17E+06	1.22E+06	
Mn-56	1.11E+05			
Mn-54	2.94E+07	2.90E+07	2.76E+07	1.31E+07
Mn-52	2.11E+05	4.34E+04	2.51E+03	
Fe-59	1.17E+09	1.07E+09	7.45E+08	4.02E+06
Fe-55	1.15E+10	1.14E+10	1.12E+10	8.90E+09
Co-60	1.09E+09	1.08E+09	1.07E+09	9.58E+08
Co-58	3.93E+04	2.52E+04	2.02E+04	1.12E+03
Cs-134	1.31E+08	1.34E+08	1.31E+08	9.36E+07
Eu-154	2.23E+08	2.21E+08	2.20E+08	2.06E+08
Eu-152	2.34E+09	2.34E+09	2.33E+09	2.22E+09

## Deposited Power Distribution in the BD BD cooling water, and BD Shielding Components

Figure 27 shows deposited power distribution in the BD and BD local shielding regions.

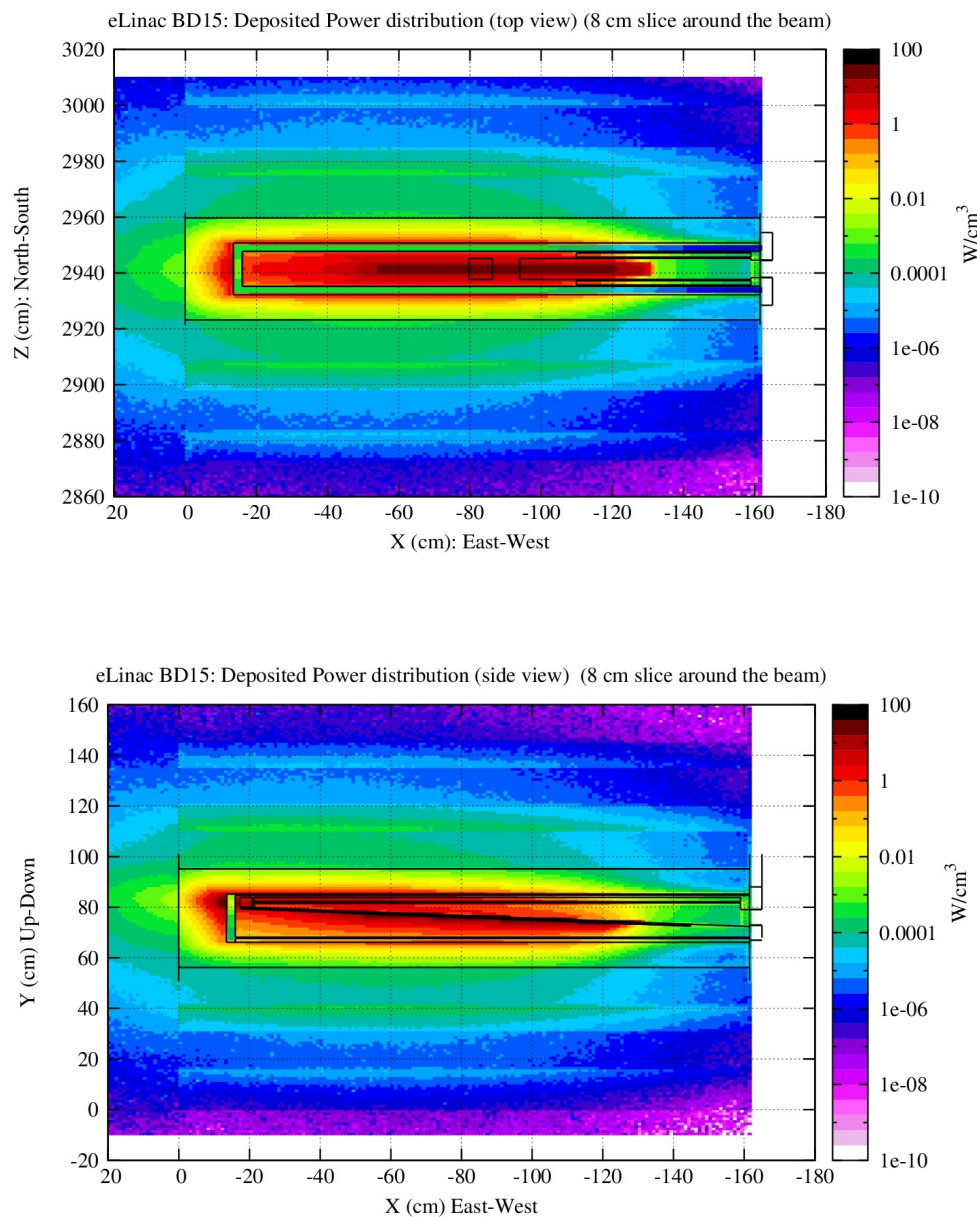


*Fig. 27: Deposited energy distribution in the BD and BD local shielding regions.  
Top: top-view, Bottom: side-view.*

Table 13 contains total deposited power in the Beam Dump Al-6061 and cooling water regions as well as in the local shilling regions. Power deposition for the 25 MeV beam is also included here for reference because of the higher power deposition in the BD Al-6061 and cooling water due to the shorter range for lower energy electrons. Range for 25 MeV electrons in Al is 4.68 cm and 10 cm for 75 MeV electrons.

*Table 13: Total power deposition.*

Region	Total Deposited Power (kW)	
	75 MeV, 1.3333 mA	25 MeV, 4mA
Al-6061	72.31	77.25
water	10.86	13.66
lead	16.65	9.04
concrete	0.04	0.013
steel	0.03	0.008
total	99.89	99.97

Power deposition was studied in more detail as input for thermal analysis of the BD and BD shielding components. BD Al 6061, cooling water, and the inner lead shielding around the BD were divided into 59 sub-regions. Sub-region designations and results are summarized in a separate report titled “100 kW eLinac BD – Power Deposition, Heat and Stress Analysis”, available on the e-Linac plane [Ref. 6].

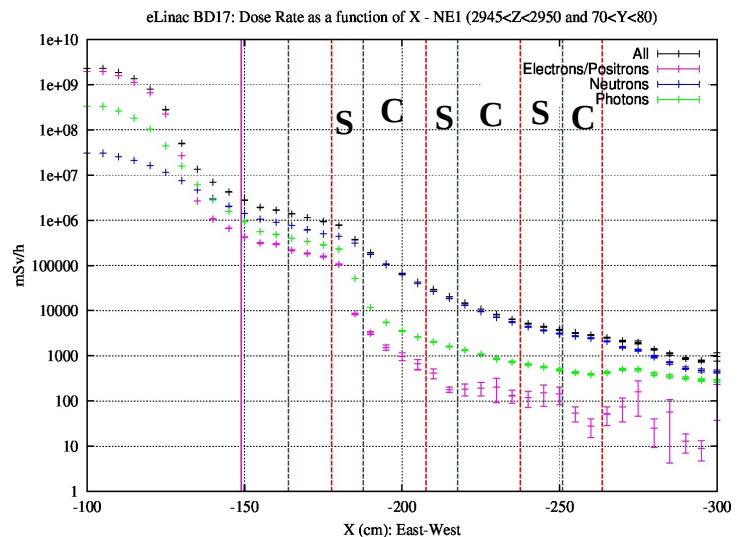
## EHDT Shielding Results – Bulk Shielding

Upstream shielding design was completed in two stages. In stage one, we filled upstream of the BD with bulk shielding along the beamline up to the available space, using a layering scheme for steel and concrete to achieve optimum attenuation, given the available space. The steel and concrete plates sit on top of a concrete support, 50 cm high.

The goal was to attenuate the upstream dose rate so that 1) laterally, the dose rate requirement of 3 mSv/h at 3 meters from the beam line center can be met and 2) longitudinally, the dose rate is reduced as much as possible to protect the upstream beamline components.

For upstream dose rates, we looked at few regions, outside of the beam pipe, on the North side. NE1 region is just outside of the beam pipe ( $2945 < Z < 2950$ ), NE2 region is 15 cm north of the beam pipe ( $2955 < Z < 2965$ ), and NE3 region is in line with the SS cut-out section ( $2975 < Z < 3085$ ). See Fig. 11 for a side-view plot of the geometry, where the three slices are visible.

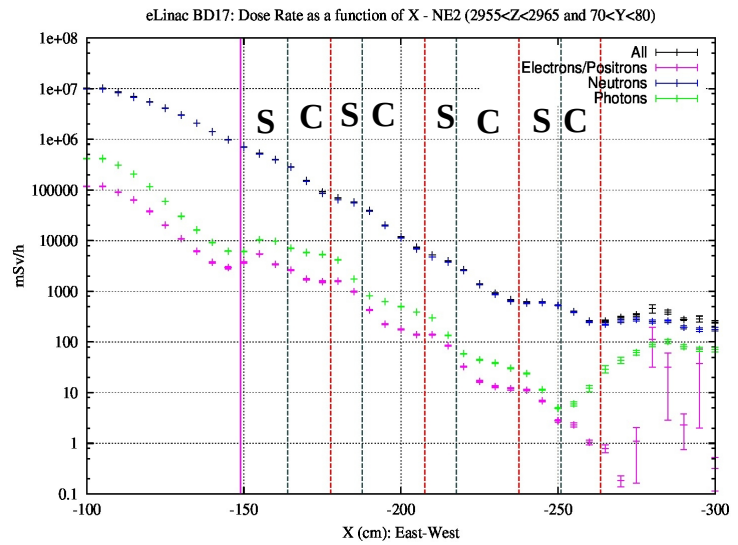
Fig. 28 shows the dose rate attenuation through the EHDT bulk shielding in the NE1 region. Magenta line indicates the upstream boundary of the BD. Blue and red lines indicate boundaries between the steel and concrete layers. The figure shows that at the entrance to the shielding, dose rate contributions from neutrons and photons are comparable but at the exit, neutrons dominate.



*Fig 28: Transmission curve through the EHDT bulk shielding in the NE1 region. Concrete and steel layers are indicated by “C” and “S” respectively. Cut-out regions filled with air are indicated with “A”.*

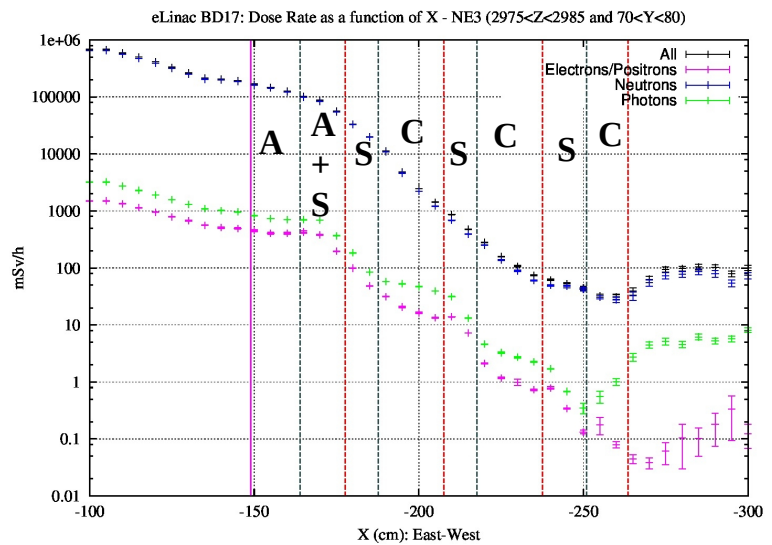
The shielding configuration achieves an attenuation of 1E3. The reason we don't observe much attenuation through the first two layers, is because in this slice there is mostly air in the first two layers due to the cut-out for the Marman clamp and other beamline components. The transmission curve through the NE2 slice will be the best representative of the dose rate attenuation through different layers of the EHDT bulk shielding. Total dose rate outside of the EHDT bulk shielding, about 1.5 cm away from the beam pipe is around 2400 mSv/h.

Fig. 29 shows the dose rate attenuation in the EHDT bulk shielding for the NE2 region. In this region (15 cm outside of the beam pipe), total dose rates outside of the EHDT bulk shielding is around 240 mSv/h. Neutrons dominate the total dose rate. The contribution from backscattered particles off of the EHDT beamline components modeled in the simulation is apparent from the increase in the dose rates in the last layer of the shielding and just outside the shielding. The observed increase in photon dose rate in the first layer of steel is believed to be due contribution from photons exiting the beam pipe at an angle.



*Fig. 29: Transmission curve through the EHDT bulk shielding in the NE2 region.*

Fig. 30 shows the dose rate attenuation in the EHDT bulk shielding for the NE3 region, which is in line with the S.S. cut-out area (see geometry in Fig. 11). Total dose rate just outside of the EHDT bulk shielding is dominated by neutrons and is around 100 mSv/h. The rise in the dose rates just outside the last concrete plate is due to backscattered particles entering the EHDT bulk shielding from upstream.



*Fig. 30: Transmission curve through the EHDT bulk shielding in the NE3 region.*

## **EHDT Shielding Results – Additional Shielding Upstream of the EHDT Bulk Shielding**

The design of additional shielding beyond the EHDT bulk shielding was the second stage of the upstream shielding design. For this stage, we made use of the two-step method as both a variance reduction tool as well as to speed up the simulation time, allowing for testing different shielding configurations upstream. To this effect, the beam pipe region was divided into two, with a boundary at the edge of the EHDT bulk shielding. Particle information (photons, neutrons, electrons, and positrons) exiting the EHDT bulk shielding and the interface between the two vacuum regions of the beam pipe were written out into files. This information was then used as the source (primaries) for the second steps, each testing different possibilities for further upstream shielding.

In the available space along the EHDT beamline, between RMH and Q6, additional collimation-style shielding was investigated. The purpose of this shielding was to further reduce the dose rates upstream, creating a 'cooler' radiation environment for the electronics and beamline equipment upstream of this shielding. Studies showed that adding 1" of lead followed by 4" of polyethylene provided sufficient shielding in the backward direction. For later phases of the ARIEL project, further shielding is necessary to reduce the dose rates down to 1 mSv/h in the south, 3 meters from the beamline center.

The possibility of adding a hutch (with walls on the top, south, and east side) as well as a wall (wall on the south side) was investigated. Results showed that for phase one, the collimation-style shielding would be sufficient and that for later phases of the ARIEL project, construction of a shielding wall would satisfy the dose rate requirement of 1 mSv/h, 3 meters south of the beamline center. Details of the dimensions and location of the collimation-style shielding and the wall are given in sec. titled "EHDT Shielding Specifications".

In the following sections, results are shown for the following simulation configurations:

- the collimation-style only
- collimator + wall shielding.
- MB4 vac. box filled with stainless steel
- MB4 vac. Box filled with vacuum
- Bore hole in the east angled wall ( $R = 5$  cm,  $L = 40$  cm).

Fig. 31 shows top and side views of the dose rate distributions upstream of the EHDT bulk shielding, with the collimation-style shielding only. Note that the MB4 vac. box was filled with stainless steel in this configuration.

Total dose rate at the CCD camera location for this configuration is around 1 mSv/h.

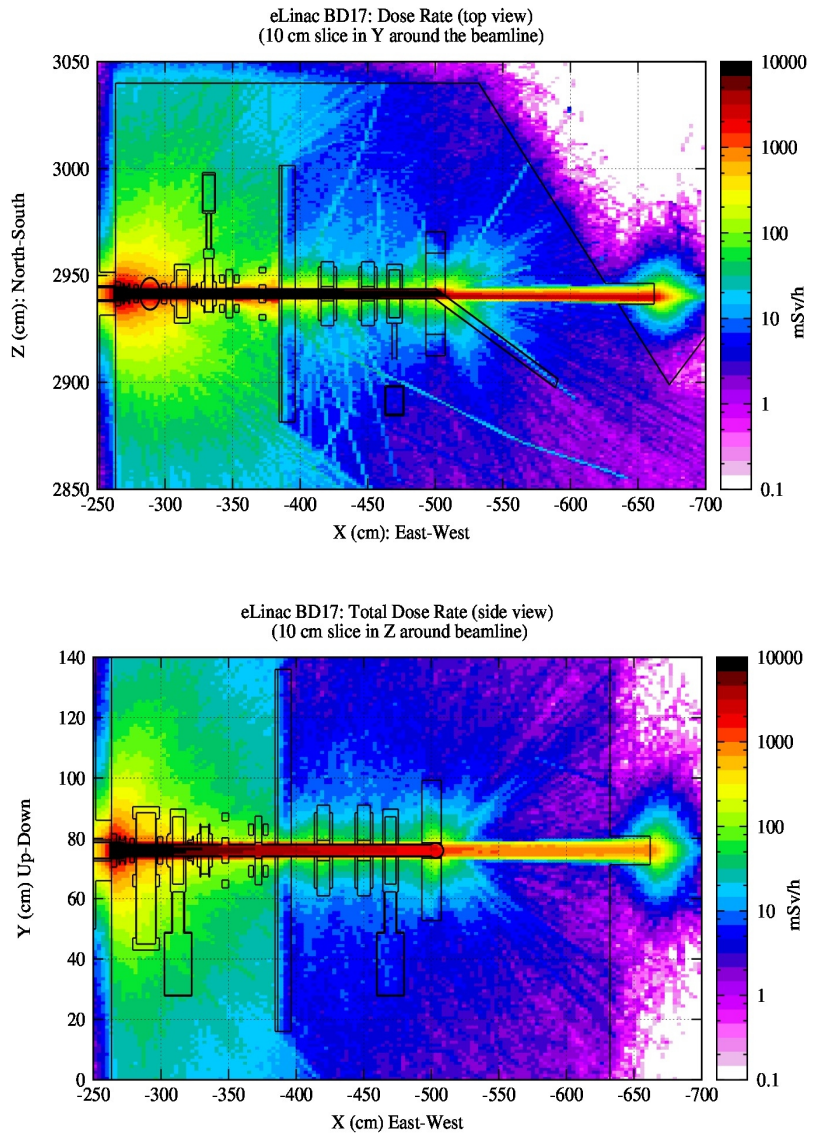


*Fig. 31: Total dose rate distributions in the backward direction, upstream of the EHDT bulk shielding with the collimation-style shielding around the beam pipe. Top: top view, Bottom: side view.*

Fig. 32 shows top and side views of the total dose rate distributions upstream of the EHDT bulk shielding with the collimation-style shielding and the wall on the south side. The MB4 vac. box was filled with stainless steel for a direct comparison with the collimator-only shielding configuration.

Without the wall, total dose rate at  $Z = 2650$  cm (3 meters from the beamline center), is 3 mSv/h. With the wall, total dose rate drops to 0.6 mSv/h.

Total dose rate at the CCD camera location for this configuration is around 0.5 mSv/h.

Assuming the worst case scenario, with the total dose rate of 1 mSv/h (and not taking into account the factor of 5 less in the conversion from ambient dose to absorbed dose for neutrons), an estimate for the life-time of the CCD and the whole camera was obtained.

The CCD camera has a radiation limit of 2-4 Gy of neutrons. This gives a lifetime of  $2\text{Gy}/(1\text{mGy}/\text{h})$  or 2000 hours.

The whole camera has a radiation limit of 20-40 Gy. This gives a life-time of  $20\text{ Gy}/(1\text{mGy}/\text{h}) = 20000$  hours.

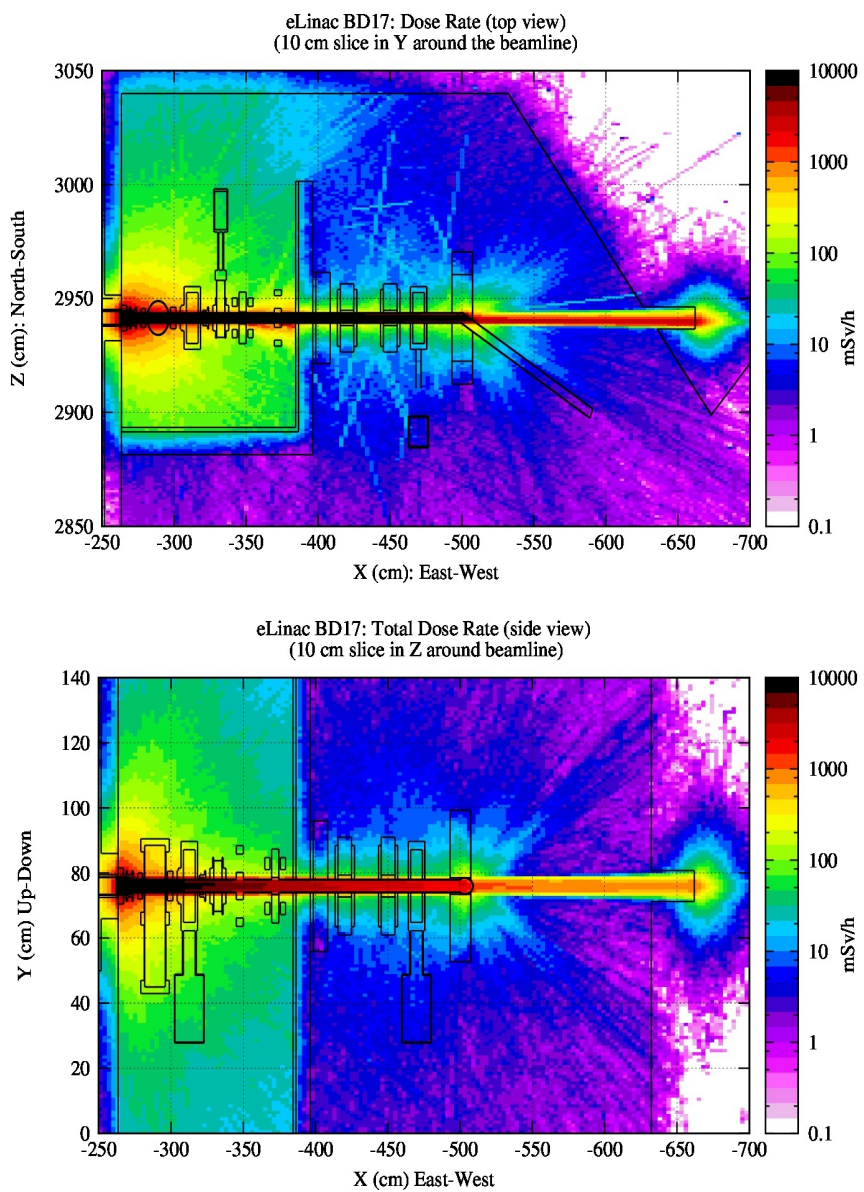


*Fig. 32: Total dose rate distributions in the backward direction, upstream of the EHDT bulk shielding with the collimation-style shielding around the beam pipe and the wall on the south side. Top: top view, Bottom: side view*

To look at the effectiveness of filling the MB4 vacuum box with stainless steel in getting the electrons to shower and in attenuating the generated photons, two configurations were investigated and compared.

Fig 33 shows the top views of the total dose rate with the MB4 vacuum box filled with vacuum (top plot) and with the vacuum box filled with stainless steel (bottom plot).

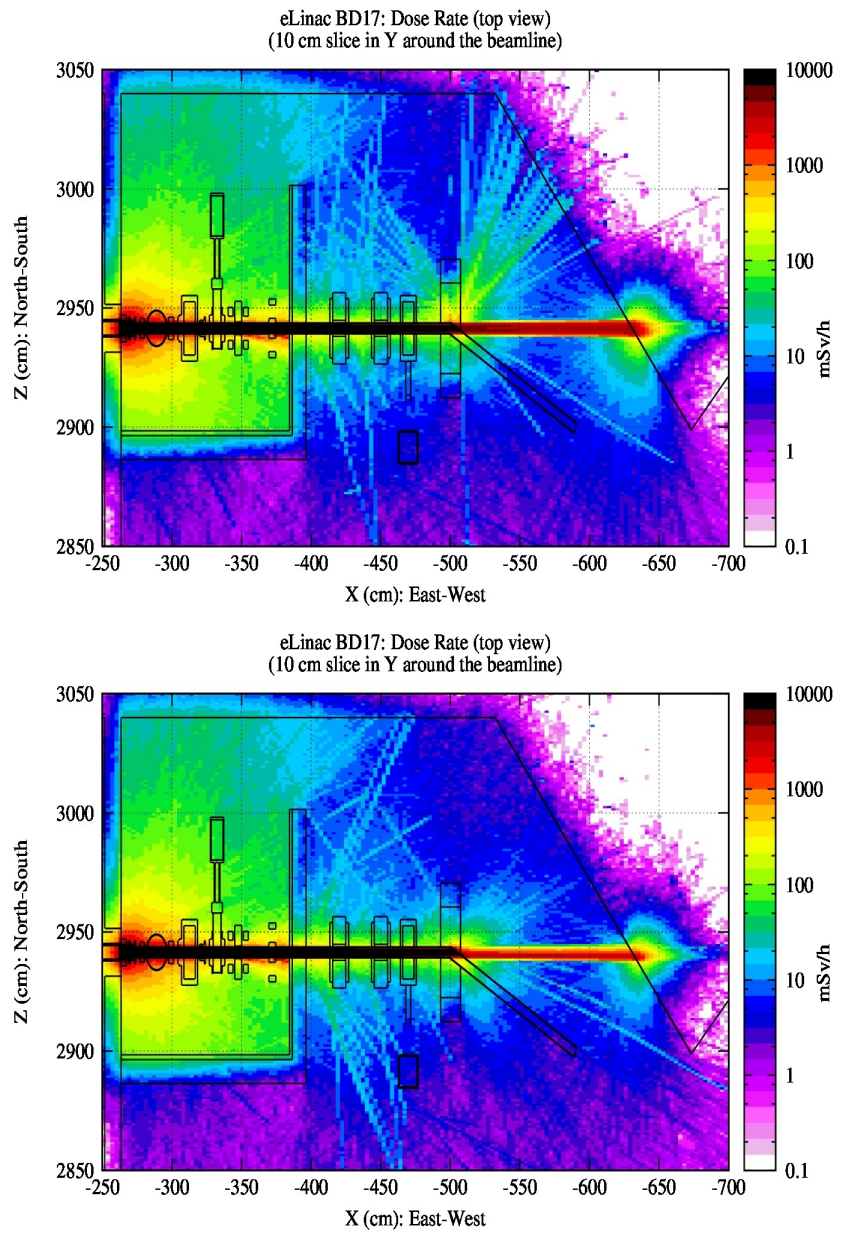


*Fig. 33: Plan view of dose rate distributions in the backward direction, upstream of the upstream bulk shielding. Top: MB4 vac. region filled with vacuum. Bot: MB4 vac. region filled with stainless steel.*

The backscattered particles inside the beam pipe are composed of mostly electrons but there are backscattered photons, neutrons, and positrons as well. Since the magnetic field in the MB4 points upward, the electrons are bent towards the North. This is apparent in top plot of Fig. 33. Stainless steel in the vacuum box, attenuates the generated photons from the electron shower in the steel (bottom plot of Fig. 33); however, the size of the shower at the MB4 location is slightly larger towards south. The back-shine at the wall from stopping backscattered particles is smaller when the vac. Box is filled with stainless steel.

To check the difference in the magnitude of the total dose rate in the wall, 1D distribution of the dose rates as a function of X was investigated. The Z and Y slices were chosen inside the beam pipe. The distributions are shown in Fig. 34.

As expected, total dose rate in the wall is less when vac. box is filled with stainless steel. Total dose rate at the entrance to the wall is  $\sim 6600$  mSv/h when the vac. box is filled with vacuum and  $\sim 3300$  mSv/h when the box is filled with stainless steel.

When looking at the dose rates in the angled east wall, it seems advantageous to fill the MB4 vacuum box with stainless steel; however, going with vacuum inside the vacuum box will also work, especially with bore hole in the east angled wall, containing the back-shine from the backscattered particles incident on the wall.

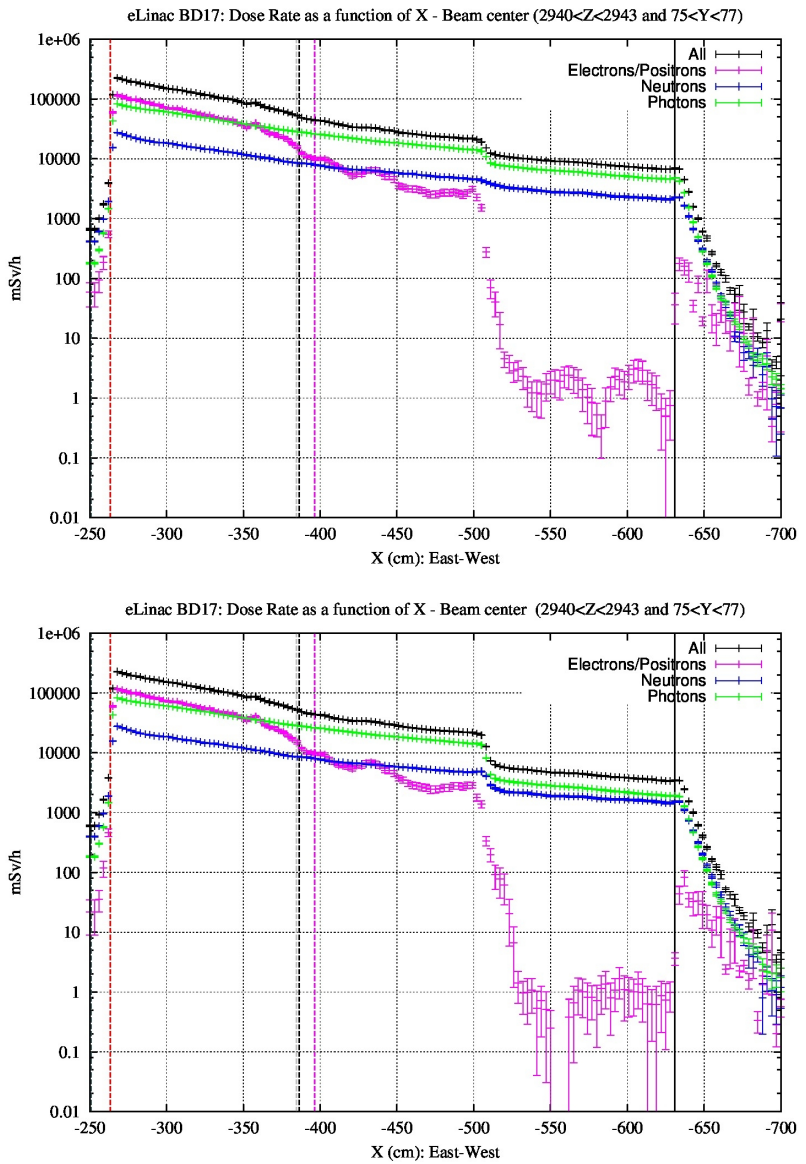


*Fig. 34: Dose rates as a function of X. Top: MB4 vac. box filled with vacuum. Bot: MB4 vac. box filled with stainless steel.*

Fig. 35 shows the top views of the total dose rate distributions for the configuration with the upstream collimator-style shielding. In both cases, there is a 5cm, 40 cm long hole in the east angled wall. The top plot shows the case when the MB4 vac box is filled with vacuum and the bottom plot is for the case when the MB4 vac box is filled with stainless steel. In the area of interest, (south east) where another CCD camera is located, the fields for both configurations are at the same level.

*Fig. 35: Plan view of the dose rate distributions in the backward direction, upstream of the EHDT bulk shielding. Note, there is no Pb/PE shielding wall on the south side.*

*Top: MB4 vac. region filled with vacuum.*

*Bot: MB4 vac. region filled with stainless steel.*

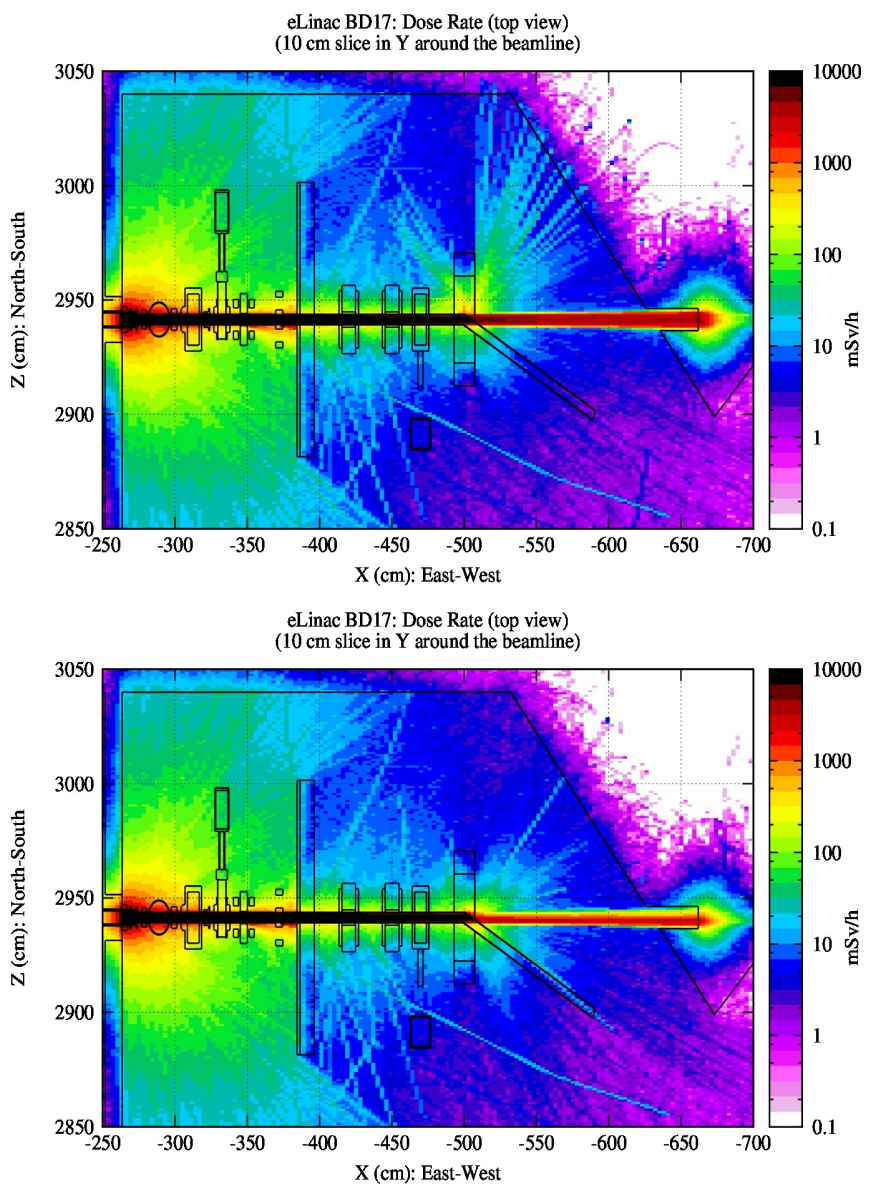


Fig 36 shows dose rate distributions as a function of Z (North\_South) and as a function of Y (Up-Down) at three upstream locations:

- 1) Just upstream of the EHDT bulk shielding,
- 2) Just downstream of the Pb/PE collimator-style shielding,
- 3) Just upstream of the Pb/PE collimator-style shielding.

These distributions are for the collimation-style only shielding around the beam pipe, i.e. with no south shielding wall. The contributions of individual particles to the total dose rate and the drop-off in the dose rates as a function of distance. Since we are not dealing with a point source, the drop-off is not expected to go as  $1/r^2$ .

Vertical blue lines indicate boundaries of the beam pipe and the vertical black line indicates the surface

of the North wall.

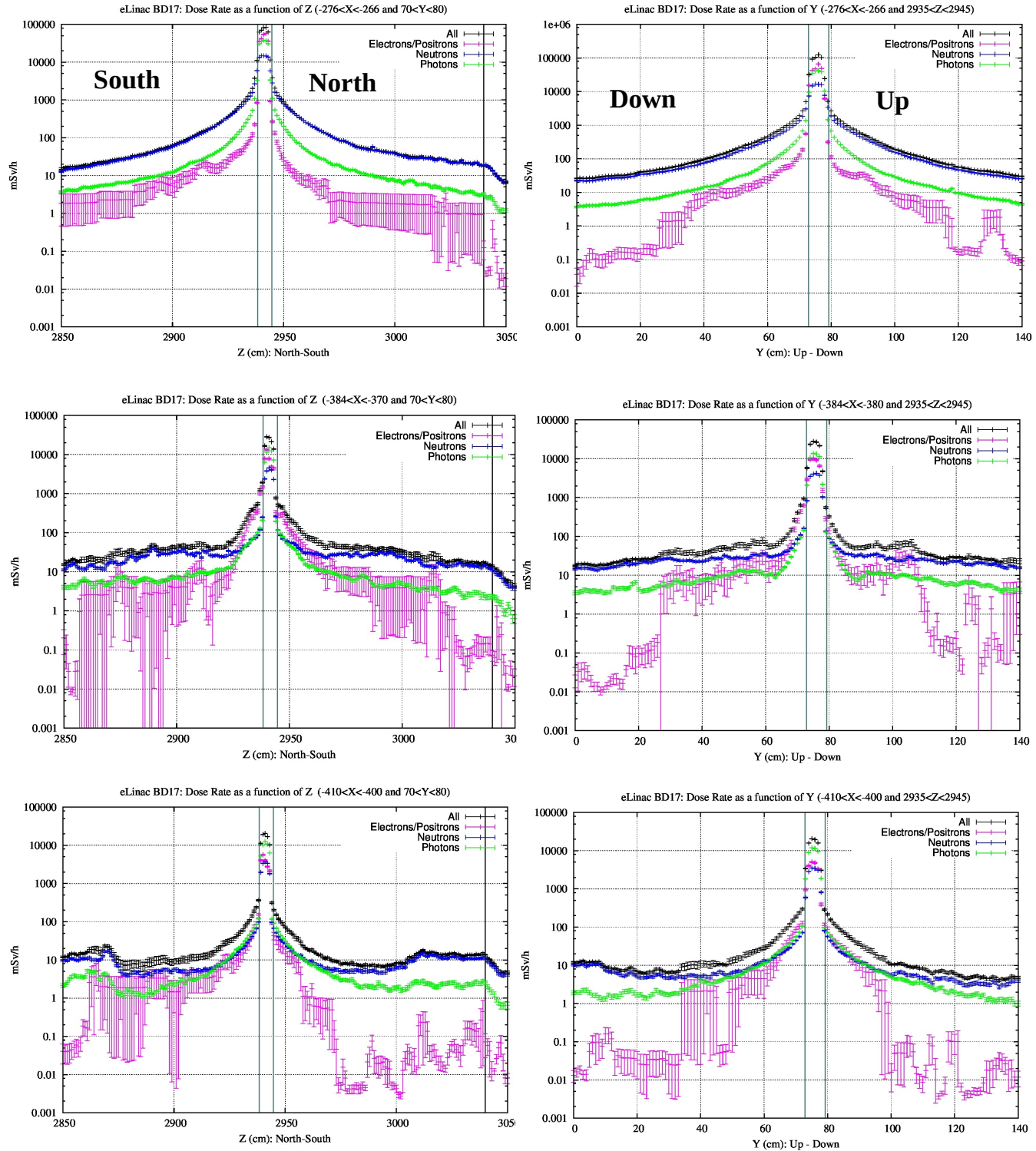


*Fig. 36: Dose rate distributions as a function of  $Z$  (left) and as a function of  $Y$  (right). Top: Just upstream of the EHDT bulk shielding. Middle: Just downstream of the Pb/PE collimation-style shielding. Bot: Just upstream of the Pb/PE collimation-style shielding.*

#### Collimator-only configuration

For comparison, the same dose rate distributions are shown in Fig. 37 for the case with the collimation-style shielding and the wall on the south side.

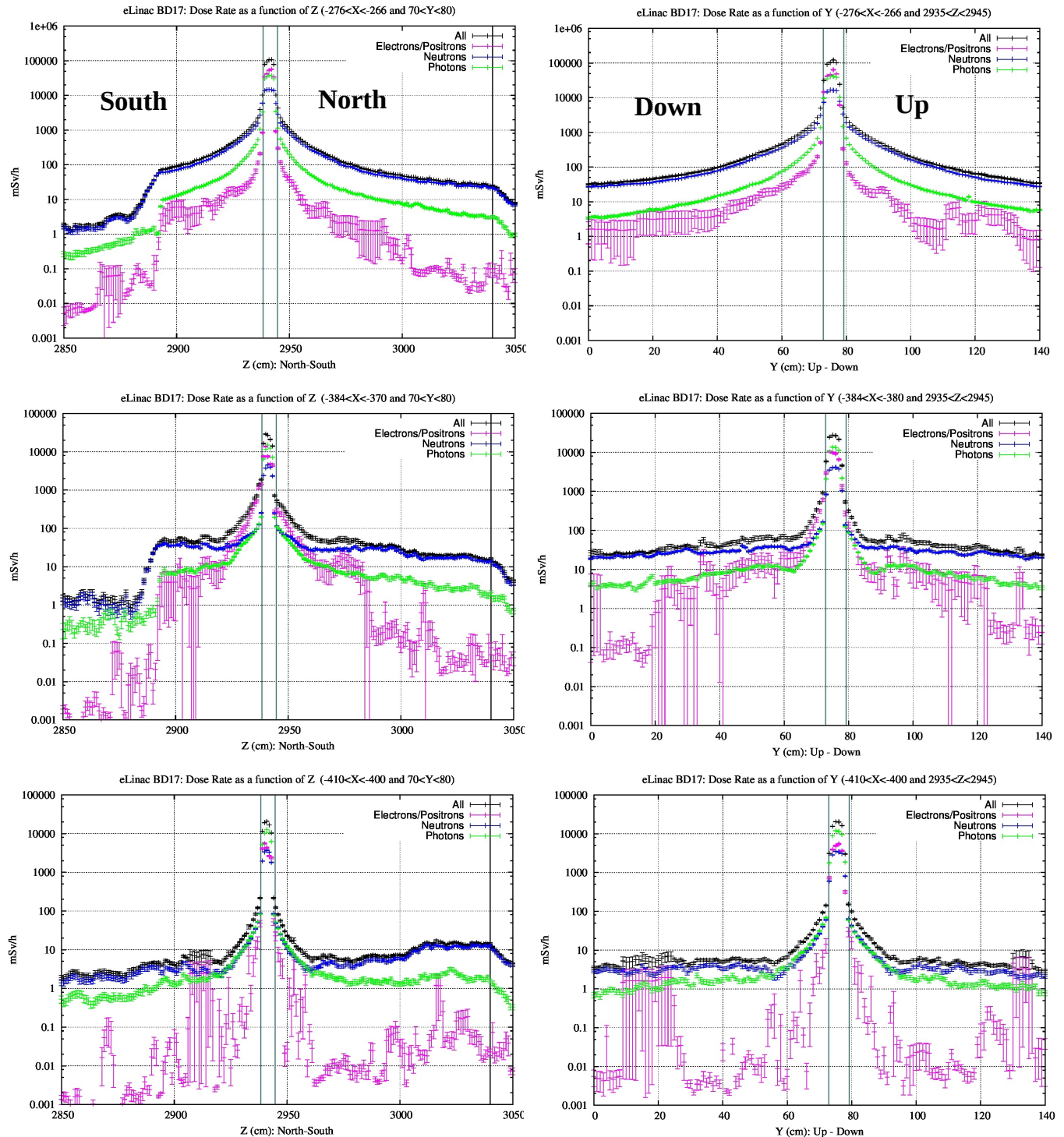


Fig. 37: Dose rate distributions as a function of Z (left) and as a function of Y (right). Top: Just upstream of the EHDT bulk shielding. Middle: Just downstream of the Pb/PE collimation-style shielding. Bot: Just upstream of the Pb/PE collimation-style shielding.

Collimator + wall configuration

The effectiveness of the wall in attenuating the dose rates is observed in plots showing the dose rate distributions as a function of Z in Fig. 37. The plots also show that neutrons dominate dose rates outside the beam pipe.

## Conclusions

A series of Monte Carlo simulations were carried out using FLUKA, to determine the shielding configuration and material for the 100 kW tuning beam dump and the upstream EHDT, located at the B2 level of the electron hall. This is where the electron gun, the injector and the first accelerator cryomodules sit. A layering scheme (alternating high and low Z material) was adopted for both the BD local and EHDT bulk upstream shielding. Studies showed this configuration to be more effective at attenuating dose rates, reducing the size/amount of shielding to meet both the dose rate requirements and the space constraints. Layers of PE and concrete proved to be the most efficient combination in reducing the dose rates to below the required limits; however, because of the high radiation environment just outside the BD, using PE was ruled out. The final materials used in the local shielding consist of an inner layer of lead followed by alternating layers of steel and concrete.

Under the 100 kW, 75 MeV electron beam operating conditions, the BD sits in very high radiation fields (1 to 100 MSv/h). This should be considered when using cables and other devices in this area. Total dose rate around the Turbo pump housed in SM6-QM is around 750 mSv/h and total dose rate around the CCD camera house in DB4 is under 1 mSv/h.

The shielding material and thicknesses specified in Table 3 for the BD meet the dose rate requirements in Table 1.

For the upstream area, additional shielding to the EHDT bulk shielding specified in Table 3 was required. A collimation-style shielding made up of lead and polyethylene, as specified on page 12, is to protect the beamline components further upstream. For future phases of the ARIEL project, a wall made up of lead and polyethylene, as specified on page 12, is necessary to reduce the dose rate to 1 mSv/h, 3 meters from the BD.

Filling the vacuum box of the MB4 magnet is beneficial in reducing the shower in the angled east wall from stopping the backscattered particles incident on the wall. Drilling a hole ( $r = 5$  cm,  $L = 40$  cm - the long edge) on the angled east wall is recommended to reduce the shine from the double-backscattered particles incident on the wall. In fact, drilling the hole in the wall, brings the radiation fields in the south east area (where another CCD camera and other beamline components sit) to the same levels as with the MB4 vacuum box filled with vacuum.

Residual dose rates 1 shift (8 hours) after EOB are around 10  $\mu$ Sv/h, 1 meters south of the outer edge of the EHDT shielding. This is an order of magnitude below the NEW limit of 100  $\mu$ Sv/h.

## Acknowledgements

This was a major project, requiring extensive amount of effort. As such, its completion would not have been possible without the contributions and collaboration of many. Thanks are due to: the 100 kW beam dump & shielding design team (Anne Trudel, Isaac Earle, Shane Koscielinak, Vance Strickland, Tim Emmens, and Eric Guetre); Ewart Blackmore, George Clark, and Kelvin Raywood for fruitful conversations and support; Curtis Baffes and Igor Rakno from Fermilab, and the FLUKA development and user community, especially Alberto Fasso, Mario Santana, Alessio Mereghetti, Vasilis Vlachoudis, and Keith Welch..

## References

1. G. Battistoni, S. Muraro, P.R. Sala, F. Cerutti, A. Ferrari, S. Roesler, A. Fasso, J. Ranft, The FLUKA code: Description and benchmarking, 2006.
2. A. Ferrari, P.R. Sala, A. Fasso, and J. Ranft, FLUKA: a multi-particle transport code, CERN-2005-10, INFN/TC\_05/11, SLAC-R-773, 2005.
3. A. Trudel & M. Nozar, 100 kW Dump Shielding Summary, July 12, 2013.
4. E. Guetre, e-Linac Electron High Energy Beam Dump (EHDT) System Requirements, Document document-104877.-57707.
4. IAEA Technical Report Series No. 188.
5. <http://elinac.triumf.ca/e-linac/wbs-areas/dump/activation-and-shielding/minas-calculations>
6. CERN yellow report 98-01.
7. L. R. Carroll, Predicting Long-Lived, Neutron-induced Activation of Concrete in a Cyclotron Vault. www.carroll-ramsey.com/conpost.pdf